Lipase catalyzed chemo-enzymatic epoxidation of fatty acids using ultrasound as a process intensification method

Master's Thesis in Chemical and Process Engineering

Pontus Lindroos

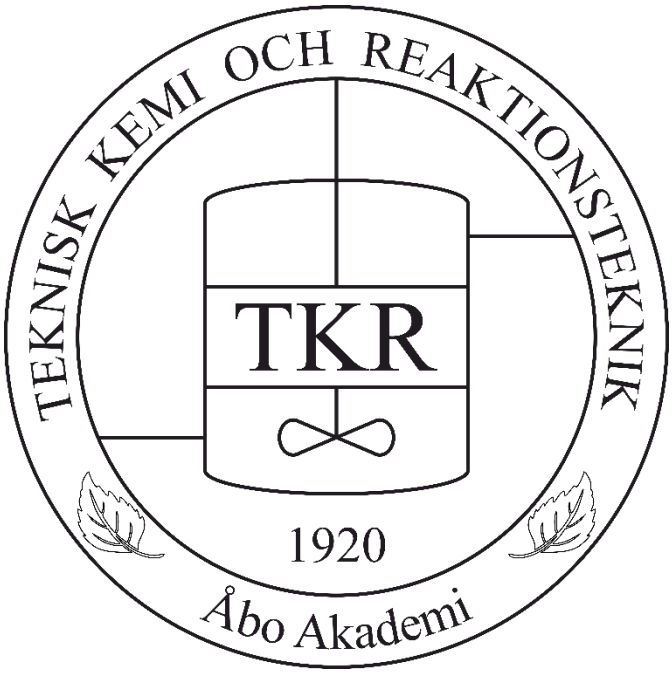

Johan Gadolin
Process Chemistry Centre

Laboratory of Industrial Chemistry and Reaction Engineering
Faculty of Science and Engineering
Åbo Akademi University
Turku/Åbo, Finland, 2021

Title of the thesis:	Lipase catalyzed chemo-enzymatic epoxidation of fatty acids using ultrasound as a process intensification method
Author:	Pontus Lindroos
Thesis supervisor:	Academy Professor Tapio Salmi *Laboratory of Industrial Chemistry and Reaction Engineering* *Faculty of Science and Engineering* *Åbo Akademi University, Turku/Åbo, Finland*
Thesis advisor:	Doctor of Technology Adriana Freites Aguilera *Laboratory of Industrial Chemistry and Reaction Engineering* *Faculty of Science and Engineering* *Åbo Akademi University, Turku/Åbo, Finland*
Keywords:	*Chemo-enzymatic epoxidation, oleic acid, immobilized lipase, process intensification, ultrasound irradiation, kinetic modelling*

Abstract

The recent trend in switching from fossil to renewable sources in the production of essential chemicals has revealed novel methods within the concept of green chemistry. This work focuses on the epoxidation of oleic acid with a chemo-enzymatic approach using immobilized lipase as catalyst. Different hydrogen peroxide versus fatty acid ratios, temperatures and stirring rates were evaluated. Acoustic irradiation was implemented for reaction intensification and different ultrasound amplitudes were studied.

The experimental results show that almost complete conversions of the double bonds in oleic acid are achievable in an isothermal batch reactor, with low concentrations of ring-opening byproducts produced. Ultrasound irradiation is used for enhancing the reaction rate, reaching high conversions in four hours of reaction time. Novozym® 435 reveals to be a working and durable catalyst for fatty acid epoxidation. The catalyst preserves its activity and selectivity well, which was confirmed by catalyst recovery experiments conducted both in a conventional batch reactor and in a sonochemical reactor in the presence of ultrasound. However, SEM images revealed that the cavitation caused by ultrasound has an impact on the catalyst morphology.

Different mathematical models for the reaction kinetics were developed and evaluated by parameter estimation using non-linear regression analysis. Statistical data for the mechanisms were evaluated and the best performing model was chosen with the chemical knowledge in mind. All the models and their estimated parameter values showed a good fit to the experimental data.

Preface

This thesis was carried out at the Laboratory of Industrial Chemistry and Reaction Engineering of Åbo Akademi University. I am pleased that I was offered the opportunity to join this excellent, international group of scientists.

Firstly, I would like to extend my deepest gratitude to my supervisor Academy Professor Tapio Salmi for offering me the thesis opportunity in this interesting research project. His advice, inspiration, and passion for science had a large positive influence on my motivation for this project. I would also like to extend my thanks to my thesis advisor D.Sc. Adriana Freites Aguilera for her continuous and extremely valuable support throughout the whole process.

Furthermore, I wish to thank Laboratory Manager D.Sc. Kari Eränen and Doctoral student Wander Pérez-Sena for their practical guidance in the laboratory. For the analytical methods of SEM, I would like to thank SEM operator Linus Silvander for the assistance. A sincere thanks also to NMR operator Ph.D. Jani Rahkila for conducting the NMR analysis.

I would also like to thank all the members of the Laboratory of Industrial Chemistry and Reaction Engineering at Åbo Akademi University for making the time at the laboratory so enjoyable and memorable. Thanks to all the fellow students as well as the student associations Kemistklubben and the Student Union of Åbo Akademi University for all the valuable and unforgettable experiences throughout the studies. Finally, I would like to thank my partner, my family, and my friends for their continuous support.

Pontus Lindroos

Helsinki, 7th April 2021

Abbreviations and nomenclature

Cat	Catalyst
CTO	Crude Tall Oil
HP	Hydrogen peroxide
N/A	Not available
NMR	Nuclear magnetic resonance spectroscopy
OA	Oleic acid
RBR	Rotating Bed Reactor
RCO	Relative conversion to oxirane (%)
RCU	Relative conversion of double bonds (%)
ROP	Ring-opening reaction
SEM	Scanning electron microscopy
TOFA	Tall Oil Fatty Acid
US	Ultrasound

A	Mass transfer area
c^*	Concentration of vacant surface sites
c_i	Concentration
IV_0	Initial iodine value
IV_{exp}	Experimental iodine value
k'	Merged rate constant
K_{Di}	Distribution coefficient
K_i	Equilibrium constant
k_i	Rate constant
m	Mass
m_{cat}	Catalyst mass
MM	Molar mass (*g/mol*)
n_{ai}	Amount of substance in aqueous phase
N_i	Molar flux
n_{oi}	Amount of substance in organic phase
OO_{exp}	Experimentally determined oxirane oxygen (*mol*/100 *g oil*)
OO_{th}	Theoretical maximum oxirane oxygen content (*mol*/100 *g oil*)
Q	Objective function
r_i	Generation rate
$s_{i,texp}$	Experimentally obtained state value
s_{it}	Computed state value
t	Time
U/g	Enzyme activity by mass
V	Volume
w/v	Weight by volume
$wt\%$	Weight percent
α	Phase ratio
ρ	Density

Table of Contents

1. Introduction

The world is currently facing a megatrend of climate change, bringing us a variety of challenges in developing novel sustainable solutions. The need for switching from fossil-based raw materials to renewables has led to discovering new techniques for producing the demanded products in the world. Non-edible plant oils are an option for the production of epoxidized oils, used as chemical intermediates for production of important products as biolubricants [1], plasticizers [2], biobased rigid foams [3], non-isocyanate polyurethanes [4], among others.

The market for oleochemical fatty acids and their derivatives has been growing in recent years, and the growth is projected to continue during the next few years [5]. The source of vegetable fatty acids can be e.g. soybean, palm, rapeseed, sunflower, linseed, and cottonseed [6]. In Northern Europe, Tall Oil Fatty Acids (TOFA) are a large and sustainable source of fatty acids. Tall oil is mainly obtained as a side product in pulping of softwood, such as pine and spruce, but also from hardwood such as birch [7], [8]. Current major players in the valorization of tall oil are Forchem, UPM Biofuels, Sun Pine and Kraton Chemical. Major investments in the field of Crude Tall Oil (CTO) refining are recently announced by Fintoil in Finland and Mainstream Pine Products in USA.

This study focuses on the chemo-enzymatic epoxidation of unsaturated fatty acids originated from renewable, plant-based resources. Oleic acid as a model molecule for fatty acids is used as feedstock for the epoxidation in this study. Moreover, in previous studies they have used other fatty acids and raw vegetable oils for the chemo-enzymatic epoxidation, such as tall oil [9], linoleic acid [10], soybean oil [11]–[13], sunflower oil [14], linseed oil [15], among others. The epoxidation reaction is catalyzed by the immobilized lipase *Candida Antarctica* lipase B on an acrylic resin support (Novozym® 435), meaning that the reaction can be carried out in mild reaction conditions with no need of an additional carboxylic acid in the reaction mixture. In this chemo-enzymatic epoxidation, only the fatty acid, an oxidant and immobilized lipase are needed for transforming the double bond of the fatty acid into an epoxy group [16].

1.1. Epoxidation of vegetable oils

1.1.1. Prileschajew epoxidation

Epoxidized vegetable oils have a great potential to replace traditional fossil-based products since they are biodegradable, renewable, and non-toxic options. For the time being, the most common method used in industrial scale for producing epoxidized vegetable oil is the Prileschajew epoxidation. This method comprises a reaction between the unsaturated fatty acid and a peroxy acid, the latter being generated *in situ* in a homogenous system with a carboxylic acid and hydrogen peroxide. Hydrogen peroxide supports the perhydrolysis of carboxylic acid in the aqueous phase, forming the percarboxylic acid for the Prileschajew epoxidation between the double bond in fatty acid and the peroxy acid in the organic phase [17]–[19]. The reaction mechanism is described in Figure 1.

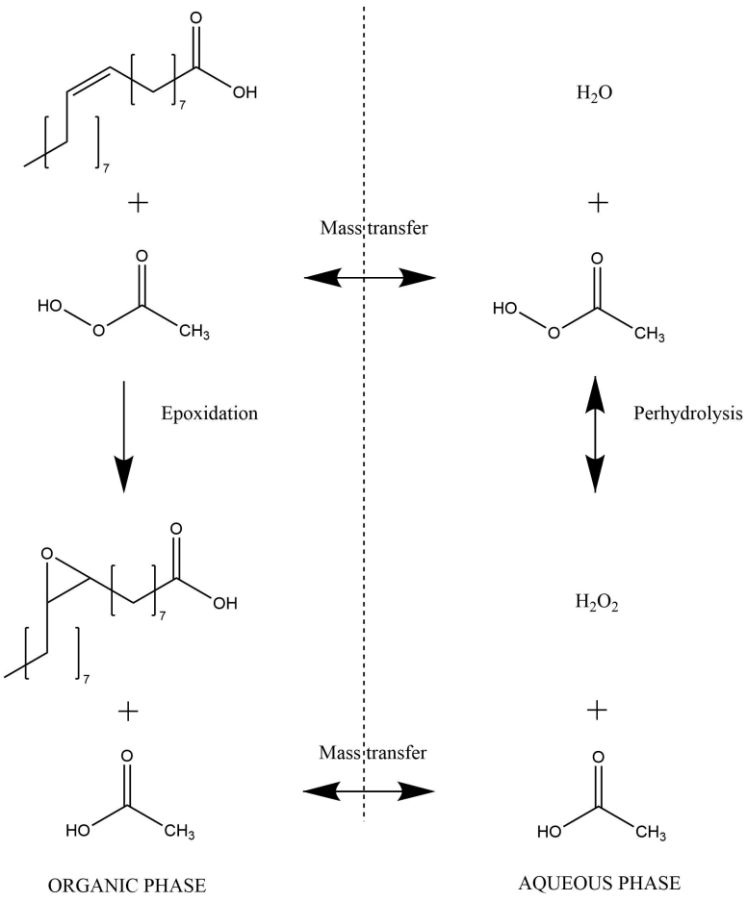

Figure 1 - The reaction mechanism for a Prileschajew epoxidation between oleic acid and acetic acid

Traditionally, strong inorganic acids such as sulfuric acid and hydrogen chloride have been used for an effective *in situ* generation of peroxy acids [20]. Subsequent studies have led to using weaker carboxylic acids such as acetic acid, as well as strong acid heterogeneous catalysts. These methods lead to a more environmentally friendly technology for the perhydrolysis step in fatty acid epoxidation. Using different kinds of acidic ion-exchange catalysts for promoting the perhydrolysis reaction in the Prileschajew epoxidation has been studied and is beneficial compared to using a pure homogenous acidic system [21], [22]. Despite being both an economical and environmentally friendly method, the epoxides produced by this Prileschajew epoxidation method are sensitive to ring-opening by nucleophiles present in the system and, therefore, the selectivity is limited [23].

1.1.2. Chemo-enzymatic epoxidation

The recent trend has switched the focus towards an enzymatic approach to epoxidation thanks to its possibilities to work in mild reaction environments by forming peroxy acids *in situ* directly from fatty acids with hydrogen peroxide as the oxidant. The concept of converting carboxylic acids and hydrogen peroxide to the corresponding peroxy acid assisted by immobilized lipases was introduced by Björkling *et al*. [24]. This was followed by Warwel and Rüsch gen. Klaas when they presented the concept of an *in situ* chemo-enzymatic 'self'-epoxidation of unsaturated fatty acids, using hydrogen peroxide and catalyzed by an immobilized lipase *Candida Antarctica* lipase B (Novozym® 435) [16], [25]. In this process, the fatty acid undergoes first a perhydrolysis step, forming together with hydrogen peroxide and lipase the needed peroxy acids. The fatty acid reacts with the peroxy acid and forms an epoxide and a fatty acid as product, supporting on the mechanism of Prileschajew epoxidation. This method consists of a liquid-liquid-solid system with hydrogen peroxide in the aqueous phase and the organic phase consisting of vegetable oil [11]. Figure 2 shows the reaction scheme of the described reaction steps for the chemo-enzymatic 'self'-epoxidation.

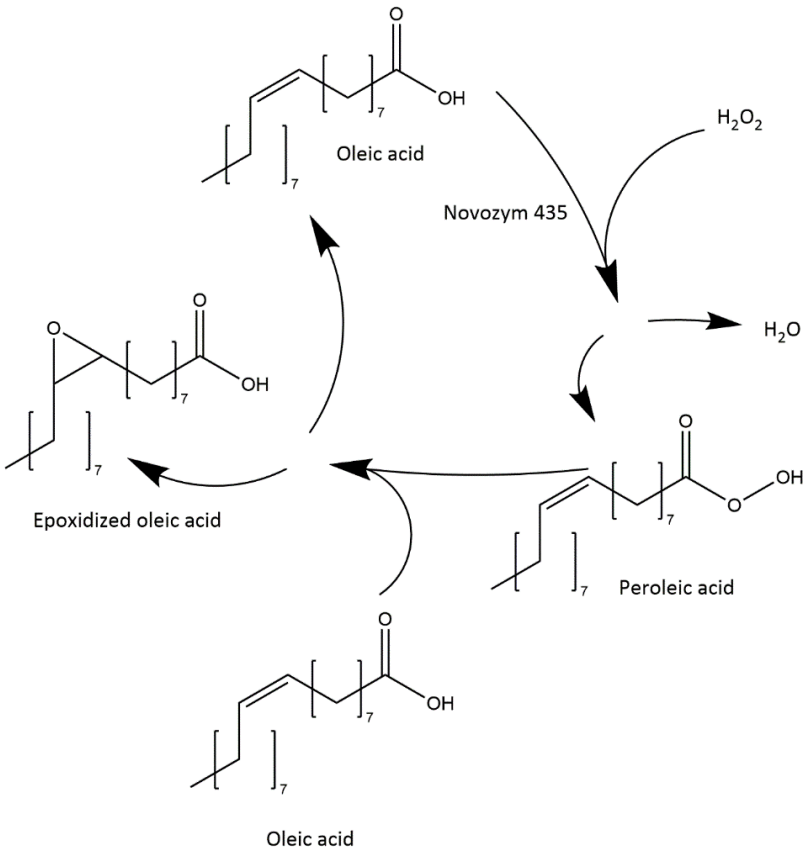

Figure 2 – The reaction scheme of chemo-enzymatic 'self'-epoxidation of oleic acid

A scenario of peroleic acid functioning as a nucleophile for another peroleic acid, thus creating an epoxidized peroleic acid as a byproduct, is worth considering in the reaction mechanism. However, due to small concentrations of peroleic acid in the reaction system, the volume of epoxidized peroleic acid produced is presumably smaller compared to epoxidized oleic acid [26].

Compared to chemical epoxidation, this chemo-enzymatic method is advantageous thanks to its low temperature conditions, higher selectivity and conversion rates [9]. The lipase has been shown to be reusable in several consecutive experiments using this method [12], [16], being an important part of making this method economically viable. Additionally, compared to the conventional Prileschajew method, this chemo-enzymatic epoxidation forms a low amount of undesired ring-opened byproducts, making this method highly selective [16].

The reaction temperature is usually a key factor for increasing reaction rates and conversions. It has been reported that the activity of immobilized lipase is impacted in temperatures exceeding 60 °C in an environment containing hydrogen peroxide and water. However, the activity is well preserved in systems without hydrogen peroxide and only water in the same temperature. This means that high concentrations of hydrogen peroxide in temperatures of 60 °C or above can have a significant damaging impact on lipase, thus leading to inefficiency [27].

In multiple studies, toluene is added as a nonpolar solvent to preserve the high levels of activity in the enzyme, protecting it from making contact with the hydrogen peroxide. This leads to an eventual increase in yield and keeps the catalyst reusable for multiple experiments [11], [12]. The use of solvents in the epoxidation reaction should, however, be carefully evaluated with the concept of green chemistry in mind [28]. The recent research studies have shown promising results for a solvent-free chemo-enzymatic epoxidation, making the process more environmentally friendly and less harmful for human health [13], [29]. The solvent polarity is, however, a governing factor for keeping the lipase activity. Water, which tends to suppress the catalytic activity, acts as a natural solvent for lipase. Therefore, the amount of water should not reach too high levels in order to preserve the efficiency of the catalyst [30].

1.2. **Process intensification in epoxidation of fatty acids**

The progression towards greener and safer solutions for producing chemicals has introduced a concept called process intensification to the list of novel technologies. Different forms of reaction intensification methods can be used, e.g. more efficient mixing and novel heating technologies. Applying an alternative form of energy to the reaction system can lead to cleaner, smaller, safer and more energy-efficient solutions for maximizing the yields [31]. Recent studies have shown favorable results for epoxidation using a combination of microwave irradiation and new forms of stirring devices, called Rotating Bed Reactors, in the epoxidation of fatty acids [32].

1.2.1. Rotating Bed Technology

When working with liquid-liquid systems where the reaction takes place in an emulsion, increasing the efficiency of the mass transfer between the two phases is key. A rotating bed reactor Spinchem® RBR is used in this study, where the packed catalyst bed is placed inside the stirring element, which aims to minimize the mass transfer limitations with a centrifugal liquid flow through the catalyst bed. The recovery of a solid catalyst from a liquid medium after the reaction can be a cumbersome procedure. By using the RBR technology, the catalyst is immobilized in the device, hence the separation process is made simpler without a need for filtration [21], [33], [34]. Figure 3 shows a schematic picture of the structure of the Spinchem® RBR device.

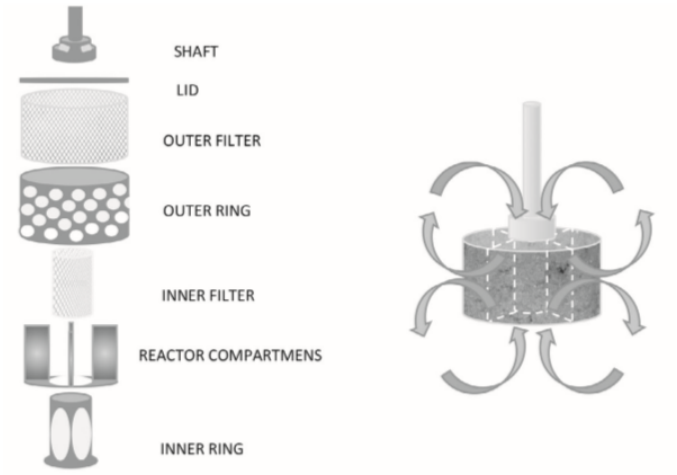

Figure 3 - A schematic view of the structure of the SpinChem RBR device and the centrifugal liquid flow [21]

1.2.2. Ultrasound irradiation

Ultrasound technology combined with conventional heating is an available option in the field of process intensification. Frequencies from 20 kHz to 10 MHz can be used in the ultrasound sonic spectrum. In contrast to using microwaves as a process intensification method, the ultrasound requires a physical medium for its application. Ultrasound in chemical reactions, also called sonochemistry, has its benefits in the form of cavitation caused by the ultrasonic waves. Small cavitation bubbles are created, growing in several cycles of compression and expansion until they eventually collapse rapidly. Consequently, high pressure and temperature peaks are generated locally with overall ambient conditions in the reactor. Free radicals can be formed in this collapse of the bubble, potentially leading to an increase in conversion in ultrasound suitable reactions [12], [31], [35]–[37]. Figure 4 shows a schematic overview of the cavitation phenomenon.

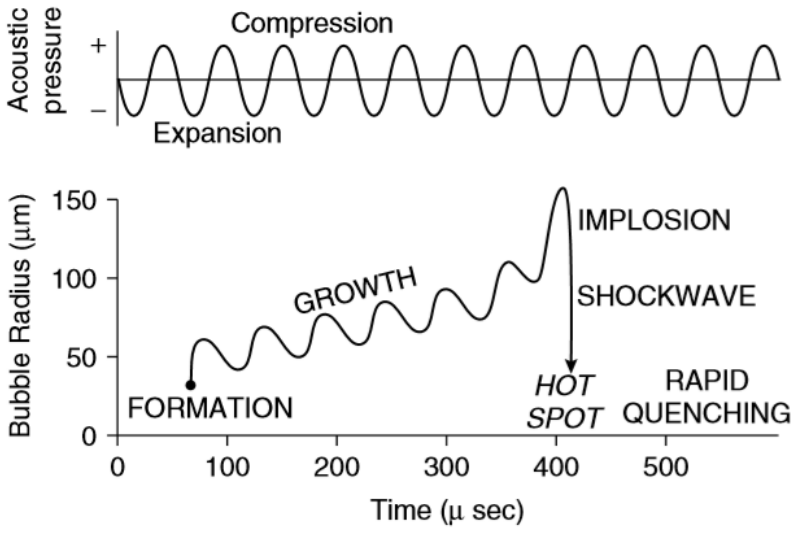

Figure 4 - A schematic overview of the cavitation phenomenon [36]

In liquid-liquid systems, ultrasound creates very fine emulsions causing an increase of the total reaction area between phases. This phenomenon is beneficial for increasing the mass transfer in the process. Furthermore, ultrasound potentially has an impact on the reaction kinetics by increasing the reaction rates [36]–[38]. The application of ultrasounds in lipase-catalyzed systems has previously shown to increase the efficiency of the enzymatic reaction without a significant decrease in the catalyst

stability. Also, morphological and structural changes of lipase can be caused by ultrasonic irradiation, leading to an increase in the surface area of the catalyst. Additionally, it has previously been shown that ultrasound has a beneficial effect on lipase activity when using ionic liquids as solvents, although, the stability is somewhat lower [30], [39], [40].

1.3. **Scope**

The purpose of this work was to study the chemo-enzymatic epoxidation of fatty acids with an immobilized lipase catalyst (Novozym® 435) in a batch reactor system. Oleic acid was used as a model molecule for fatty acids and the initial molar ratios of hydrogen peroxide versus fatty acid were optimized. Ultrasound as a process intensification method was introduced and studied further. The work consisted of the following tasks:

- Optimization of the molar ratio of unsaturated fatty acid to hydrogen peroxide in silent mode at different reaction times
- Introduction to sonochemical reactors using ultrasound irradiation, comparing different ultrasound amplitudes and their impact on the reaction rate and reactant conversion
- Investigation on the influence of the temperature and the stirring speed in the chemo-enzymatic epoxidation conducted under ultrasound irradiation
- Study of the possibilities for reusing the catalyst in several consecutive experiments in both conventional and sonochemical reactor environments
- Development of a mathematical model for the reaction in a conventional reactor environment, including simulation and parameter estimation for the description of the reaction kinetics

2. Experimental

2.1. Chemicals utilized

A list of the chemicals and the manufacturers used for this project are provided in Table 1 below.

Table 1 - List of chemicals utilized for the reaction and analysis

Chemical	Purity	Manufacturer
Oleic Acid	90%	Sigma-Aldrich
Lipase acrylic resin (Novozym 435)	≥5.000 U/g	Sigma-Aldrich
Hydrogen peroxide	>30% w/v	Fischer Scientific
Tetraethylammonium bromide	98%	Sigma-Aldrich
Perchloric acid (in anhydrous acetic acid)	0.1 M	VWR chemicals
Potassium iodide	N/A	Merck KGaA
Sodium thiosulfate solution	0.1 M	Honeywell Fluka™
Hanus solution	N/A	Merck KGaA
Chloroform	≥99.8%	Honeywell Riedel-de Haën™
Ammonium cerium sulfate solution	0.1 M	Honeywell Fluka™
Acetic acid	≥99.8%	Sigma-Aldrich
Ferroin indicator	N/A	VWR chemicals
Toluene	≥99.9%	Honeywell Riedel-de Haën™
Sulfuric acid	95-97%	Sigma-Aldrich
Starch	N/A	Merck KGaA

2.2. **Experimental setup**

2.2.1. Reactor setup

All experiments were performed in a 250 ml isothermal batch glass reactor vessel surrounded by a thermostatic jacket (Lenz®). The jacket was filled with a mixture of ethylene glycol which was heated by a circulation bath assisted by a conventional heat exchanger. The reactor was equipped with a reflux condenser for preventing the evaporation of the volatile compounds in the reaction mixture during the reaction process.

The formation of an emulsion during the reaction was made by stirring with a rotating bed reactor system (SpinChem® RBR) placed inside the reactor vessel (Figure 5). The RBR consisted of four rotating catalyst bed chambers, where the solid catalyst could be placed, which enabled the use of immobilized solid catalyst without any need of separation of the catalyst from the reaction mixture. In this setup, the reaction system undergoes a centrifugal effect, pushing the inner parts of the mixture to the outer parts of the reactor [33]. The SpinChem® device was used with the catalyst inside and outside the chambers. The ultrasound experiments were conducted with an ultrasound horn (microtip, Fischerbrand®) inserted in the glass reactor. Different amplitudes of the ultrasound microtip, 30%, 60% and 90%, with a frequency of 20 kHz were used during the experiments. The temperature was continuously recorded during the experiments by the software Picolog® connected to a thermocouple that was protected by Teflon and inserted in the reactor. A 10 ml syringe was used for withdrawing samples. Images of the reactor equipment can be found in Appendix I.

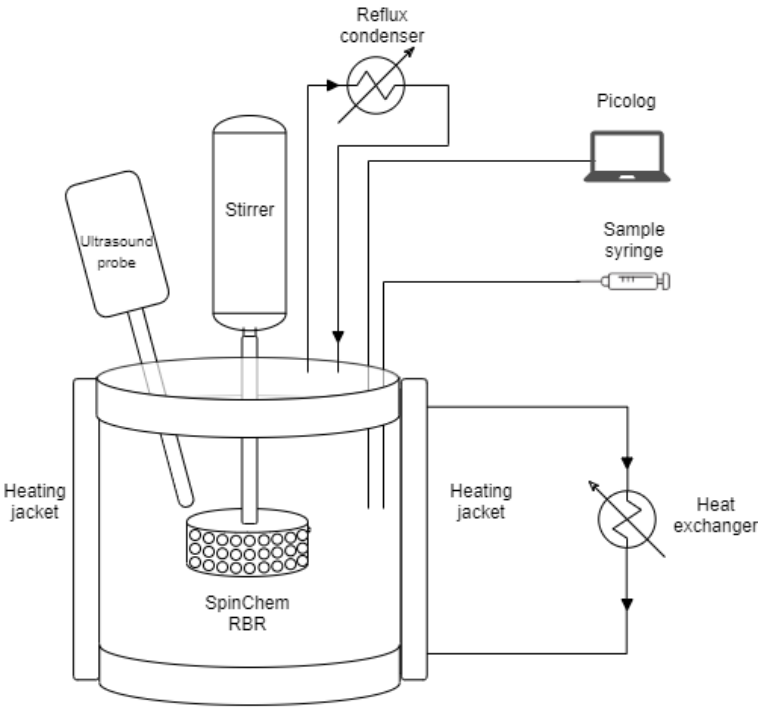

Figure 5 - Scheme of the reactor setup

2.2.2. Experimental matrix

The experiments were performed in seven different experimental sets, three sets conducted in the absence of ultrasound and four sets with ultrasound. To obtain an understanding of the optimal molar ratio of unsaturated fatty acid versus hydrogen peroxide, the epoxidation process was at first optimized under silent conditions without using ultrasound as process intensification method. With the optimal oleic acid to hydrogen peroxide ratio determined in silent mode with the first seven experiments, the same conditions were used in experiments assisted with ultrasound. In the experimental sets with ultrasound, the amplitude of ultrasound, temperature and stirring rate was adjusted to find maximal conversions and reaction rates. The experiments and their reaction conditions are listed in Table 2.

Table 2 - Experimental matrix

Experiment number	*Ultrasound amplitude (%)*	*Catalyst load (%)*	*OA:HP ratio (mol:mol)*	*Temperature (˚C)*	*Time (h)*	*Stirring speed (rpm)*	*Remark*
1	-	7.00	1:1.5	50	6	1000	SpinChem used
2	-	7.00	1:1.5	50	6	1000	
3	-	7.00	1:1	50	6	1000	H_2O_2
4	-	7.00	1:2	50	6	1000	amount
5	-	7.00	1:1.75	50	6	1000	testing
6	-	7.00	1:2	50	12	1000	
7	-	7.00	1:1.5	50	12	1000	
8	0	7.00	1:2	50	8	1000	Testing
9	30	7.00	1:2	50	8	1000	US
10	60	7.00	1:2	50	8	1000	amplitude
11	90	7.00	1:2	50	8	1000	
12	90	7.00	1:2	30	8	1000	Testing
13	90	7.00	1:1.75	45	8	1000	temperature
14	90	7.00	1:2	60	8	1000	
15	90	7.00	1:2	60	8	500	Testing
16	90	7.00	1:2	60	8	750	stirring speed
17	-	7.00	1:1.5	50	8	750	Lipase
18	-	7.00	1:1.5	50	8	750	reusability
19	-	7.00	1:1.5	50	8	750	-silent
20	90	7.00	1:1.75	50	8	750	Lipase
21	90	7.00	1:1.75	50	8	750	reusabilty -
22	90	7.00	1:1.75	50	8	750	ultrasound

2.2.3. Experimental procedure

All the experiments were performed in batch mode. The oleic acid, lipase (Novozym 435), hydrogen peroxide and water were measured up in separate Erlenmeyer flasks or glass beakers covered with paraffin film. For the experiments where the SpinChem® was used as a rotating catalyst bed, the catalyst was distributed evenly in the four different chambers and the lipase filled device was placed in the reactor before adding any reactants. In the other cases, the catalyst was weighed in a beaker with the same procedure as the reactants and the SpinChem® was inserted empty, working only as a stirrer.

Oleic acid, water and lipase were added into the reactor and the stirring device was switched on with the desired speed to create the emulsion. After the reactor reached the desired temperature of the experiment, hydrogen peroxide was added dropwise during about one-minute time, in order to prevent both an impact on the stability of lipase and an undesired rapid exothermic reaction, where a temperature peak is created. The time-point when hydrogen peroxide was added into the mixture was considered as the start of the reaction. When conducting an ultrasound experiment, the ultrasound horn was turned on after all the reagents were added and the operating cycle of the device was 1 minute ON and 1 minute OFF throughout the experiment.

After the reaction was stopped, the stirring was shut down and the emulsion was left for 10 minutes to spontaneously separate in two phases. The aqueous phase was carefully withdrawn from the reactor through a drain, and toluene was added to the remaining organic phase in order to handle it more easily. The catalyst was recovered by a vacuum filter and further washed with toluene to clean possible remaining products on the enzyme. After air drying the catalyst in a fume hood for 12 hours, it was used for the next reaction when the reusability of the lipase was studied.

2.3. **Analytical procedures and methods**

The sampling was done mainly every hour except for the 8-hour and 12-hour experiments where also two-hour intervals were used in the later part of the reaction. The samples with a volume of 5 ml were withdrawn with a syringe through a Teflon®-coated sampling tube. The sample was left in the sampling syringe for a few minutes to separate in two phases before placing in two sample bottles for analysis: one bottle for the aqueous phase and one for the organic phase. Both bottles were placed in a centrifuge for two minutes, in order to separate the solid catalyst particles from the samples. The aqueous phase was analyzed immediately to prevent any decomposition of hydrogen peroxide. The organic phase was transferred to an oven at 60 ˚C, ensuring a homogeneous sample and preventing any solidification. Two different analyses were carried out for the organic phase, one directly after sampling, another after being stored 12-72 hours in the freezer. Images of the titrimetric analysis equipment is found in Appendix I.

2.3.1. Aqueous phase analysis – Hydrogen peroxide content

The aqueous phase samples were analyzed within 30 minutes after withdrawal. The concentration of hydrogen peroxide was analyzed by the Greenspan and MacKellar method [41]. This was done by measuring 0.1 g of sample in an Erlenmeyer flask, diluted in 50 ml of 10% sulfuric acid and adding three drops of ferroin indicator. Then 1-2 ice cubes were added in the flask to decrease the temperature below 10 ˚C for the titration of the solution with ammonium cerium sulfate. The solution was titrated under stirring from orange color to transparent. The amount of hydrogen peroxide in the aqueous phase was calculated as follows:

$$wt\ \%\ H_2O_2 = \frac{[]_{cerium} V_{cerium} M_{H_2O_2} * 100}{2 * m_{sample}} \qquad (1)$$

2.3.2. Organic phase analysis – Iodine value

The iodine value describes the number of double bonds in a sample, expressed as grams of iodine reacted in 100 g of oil. The analysis was conducted by applying the Hanus method [42]. For this analysis, 0.1 g of organic phase was measured up in an Erlenmeyer flask, dissolved in 20 ml of chloroform and 20 ml of Hanus solution (iodine bromide in acetic acid). The flask was left for one hour in a dark place for the iodine to completely react with the double bonds in the sample. After one hour, 20 ml of 10% potassium iodide solution were added to let the remaining iodine bromide react, and 100 ml of water was added to clean the walls of the flask. A small amount of starch indicator was added, and the whole mixture was titrated under stirring with a 0.1 M sodium thiosulphate solution until the solution turned transparent. The volume of titrator solution spent for analyzing the sample was used for calculating the iodine value:

$$IV = \frac{[\,]_{Na_2S_2O_3} * (V_{Blank} - V_{sample}) * MM_I * 100}{m_{sample}} \quad (2)$$

This can be transformed into relative conversion of double bonds (RCU) as follows:

$$\%RCU = 100 - \left(\frac{IV_0 - IV_{ex}}{IV_0}\right) * 100 \quad (3)$$

where IV_0 is the initial iodine value of the organic sample and IV_{ex} the iodine value for the particular experiment.

2.3.3. Organic phase analysis – Oxirane number

Jay's method was used to determine the amount of oxirane groups (epoxy groups) in the organic phase [43]. In the analysis, 0.1 g of organic phase sample were dissolved in 10 ml of chloroform and 10 ml of 20 wt% tetraethyl ammonium chloride (TEAB) dissolved in acetic acid. The mixture was titrated with 0.1 M perchloric acid in acetic acid using an automatic potentiometric titrator (799 GPT Titrino, Metrohm, recorded with the software tiamo™). The conversion to epoxy groups can be expressed as the relative conversion to oxirane (RCO) calculated from,

$$\%RCO = \frac{OO_{ex}}{OO_{th}} * 100 \quad (4)$$

where OO_{ex} is the experimentally determined content of oxirane oxygen, and OO_{th} the theoretical maximum oxirane content in 100 g of oil. The theoretical maximum OO_{th} was calculated from:

$$OO_{th} = \left(\frac{{}^{IV_0}/_{2MM_i}}{100 + \left({}^{IV_0}/_{2MM_i}\right) * MM_0} \right) * MM_0 * 100 \quad (5)$$

where MM_i is the atomic mass of iodine, and MM_O the atomic mass of oxygen.

2.3.4. Nuclear Magnetic Resonance spectroscopy (NMR)

For the analysis of products in the organic phase, a Bruker AVANCE III spectrometer operating at 500.10 MHz (^{1}H) equipped with a BB/1H SmartProbe was used. All samples were dissolved in deuterated methanol-d4 and the spectra were recorded at 25 °C.

2.3.5. Scanning Electron Microscopy (SEM)

Scanning Electron Microscopy (SEM) was used for studying the morphology of the catalyst, with a particular focus on the cavitational effects of ultrasound on the catalyst material. The equipment used was of model Zeiss Leo Gemini 1530. The images were taken at 30x, 100x, 250x and 1000x.

3. Results and discussion

3.1. SpinChem® Rotating Bed Reactor

All experiments except one were conducted by adding the catalyst to the reaction mixture. Using the SpinChem® RBR as a rotating catalyst bed device turned out to be insufficient due to accessibility problems, hypothetically caused by the high viscosity of oleic acid and the relatively high amount of immobilized lipase packed in the device. As shown in Figure 6, parts of the catalyst bed remained dry and consequently the efficiency of the enzymatic catalysis in this system was strongly suppressed.

Regardless of this, the SpinChem® RBR showed to be an efficient stirrer when the catalyst was added directly in the mixture. One hypothesis for the good efficiency is that the immobilized lipase is preserved better when using SpinChem® RBR as a stirrer instead of traditional agitators, that can have a grinding effect on the catalyst [34].

Figure 6 – Novozym® 435 in the SpinChem® RBR after using as a rotating catalyst bed

3.2. **Determination of optimal reaction parameters**

3.2.1. Influence of hydrogen peroxide

The influence of different hydrogen peroxide molar ratio versus unsaturated fatty acid ratio was studied extensively. Molar ratios (oleic acid to hydrogen peroxide, later OA:HP) of 1:1, 1:1.5, 1:1.75 and 1:2 were studied. All the experiments in this section were conducted with a hydrogen peroxide solution of 30% w/v without the assistance of ultrasound. A catalyst load of 7% w/w with respect to the oleic acid mass was used at 50 ˚C, 1000 rpm with the SpinChem® RBR. The durations of the experiments were 6 and 12 hours.

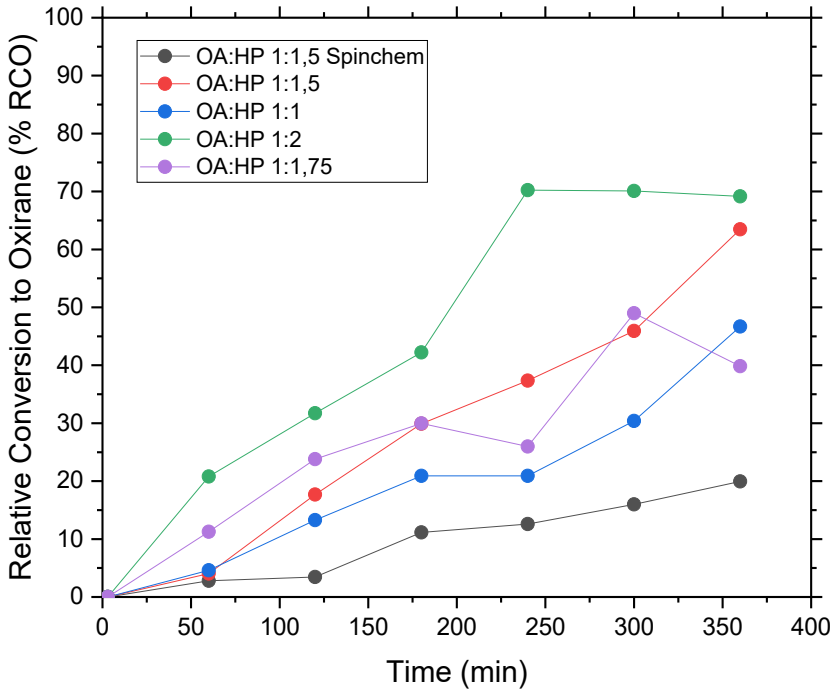

Figure 7 - Relative conversion to oxirane (RCO) for different OA:HP molar ratios during 6 hours in silent mode

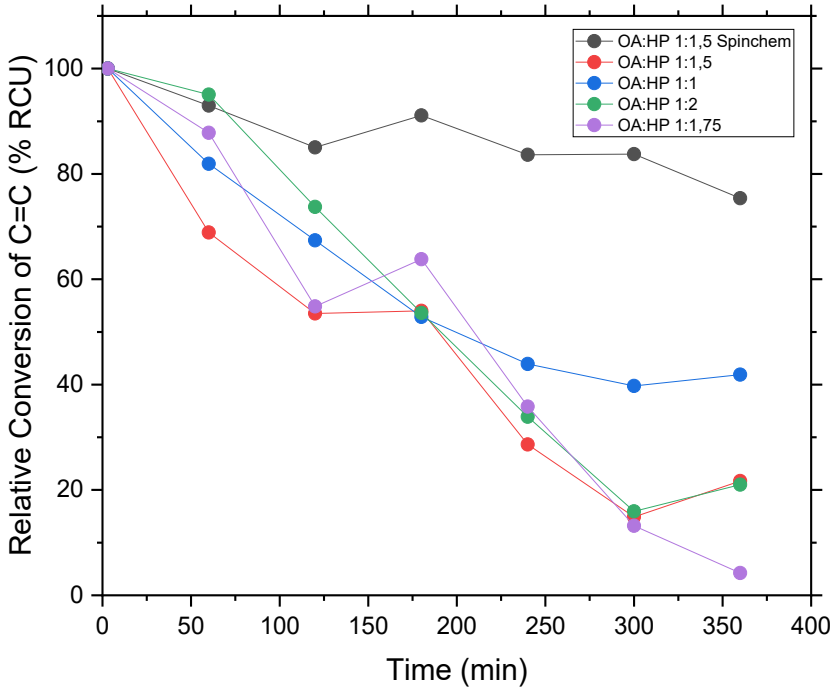

Figure 8 - Relative conversion of double bonds (RCU) for different OA:HP molar ratios during 6 hours in silent mode

Figure 7 and Figure 8 show that the highest conversions to epoxide were reached more rapidly with higher ratios of hydrogen peroxide, the RCO of 81 % was reached after 4 hours in the experiment with OA:HP 1:2 ratio. A consistent decrease in the reaction rate can be seen with the experiments closer to equimolar levels of hydrogen peroxide versus unsaturated fatty acid. However, by comparing Figure 9 with Figure 7, a ratio of OA:HP 1:1.5 reached slightly higher levels of epoxide after 8 hours with equivalent reaction conditions. A remarkable fact is also that even at the lowest OA:HP ratio, 1:1, the reaction rate is on steady levels still after 6 hours (Figure 7), meaning that higher yields are possible to reach by increasing the reaction time. Considering both economic and environmental aspects, optimizing the process with a lower amount of hydrogen peroxide is a good consideration since feasible levels of epoxide yield can still be reached.

For the Prileschajew epoxidation method used in industrial-scale processes, side-reactions in the form of ring-opening are observed [8], [21], [23]. In this work, using a chemo-enzymatic epoxidation method, there is a quantitative difference between the measured values of epoxy groups and the converted double bonds in the fatty acid. This indicates the formation of ring-opening products (Figure 9). The presence of ring-opening products was further studied with NMR analyses, which are discussed in section 3.4.

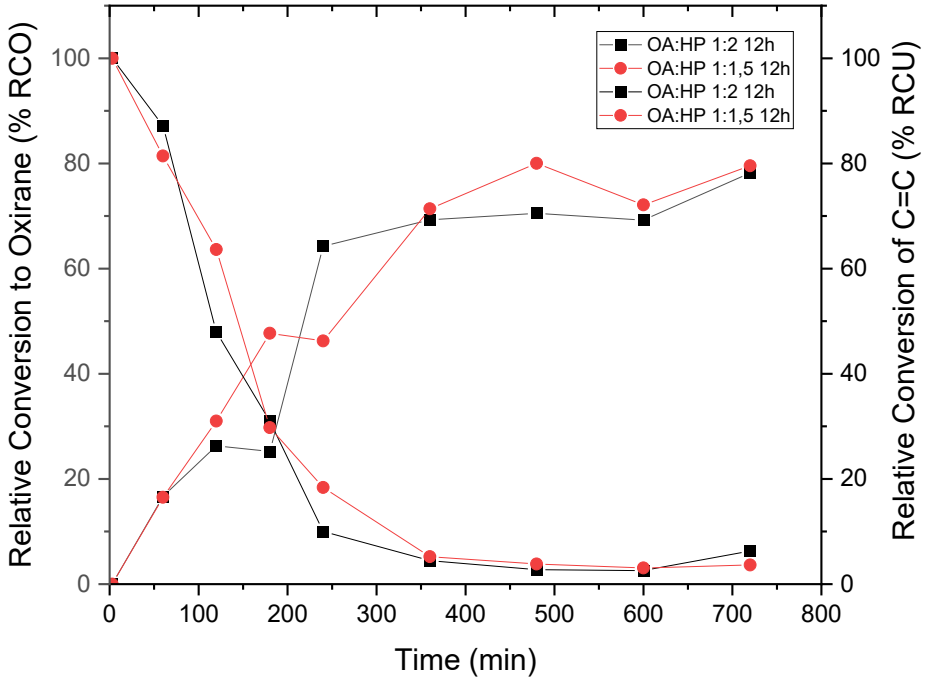

Figure 9 - Relative conversion to oxirane (RCO) and double bonds (RCU) for different OA:HP molar ratios during 12 hours in silent mode

Törnvall *et al*. reported that high amounts of hydrogen peroxide in temperatures above 20 ˚C impair the activity of lipase, hence lower conversions are obtained [27]. However, in this work, no major decrease of the catalyst activity was detected when higher ratios of hydrogen peroxide were used. Since a relatively low concentration of 30 % w/w hydrogen peroxide solution was used in all the experiments, the catalyst activity might not have been influenced by hydrogen peroxide. For further investigation on the impact of hydrogen peroxide on the lipase catalyst, higher concentrations of hydrogen peroxide could be tested at equivalent reaction conditions.

3.2.2. Influence of ultrasound

One of the main goals for this work was to study the influence of acoustic cavitation in the form of ultrasound irradiation. The ultrasound probe was operated at a frequency of 20 kHz at different amplitudes of 30%, 60% and 90%, with a power output of 22 W, 28 W and 34 W, respectively. For keeping the isothermal conditions in the system, a duty cycle of 50% was used, meaning that the ultrasound probe was switched on for one minute, whereafter the probe was switched off for one minute. At a catalyst load of 7 wt%, a fatty acid to hydrogen peroxide ratio of 1:2, 50 ºC and a stirring speed of 1000 rpm were utilized.

Four experiments with identical reaction conditions, but with varying amplitudes of 30%, 60% and 90% were conducted in this set. A reference experiment was performed with the ultrasound probe in the reactor in the absence of ultrasound. As depicted in Figure 10, the results show clear indications of a positive effect on the reaction rates compared to the experiments in silent conditions.

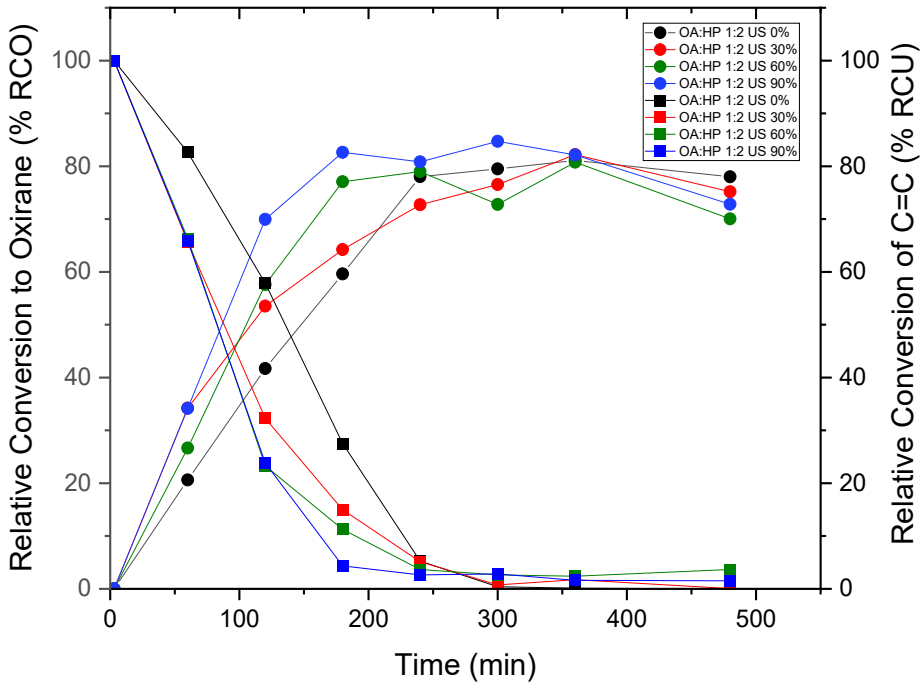

Figure 10 - Relative conversion to oxirane (RCO) and double bonds (RCU) for different ultrasound amplitudes during 8 hours

As reported by Bhalerao *et al*., a continuous increase in the reaction rate can be observed by increasing the input power of ultrasounds [12]. A similar effect was confirmed by the experiments in this study, since an amplitude of 90% resulted in the highest RCO levels, at 84% after three hours. Considering the financial aspects in the use of ultrasound equipment, the results of RCO 80% after three hours with 60% amplitude can be considered as competitive as the results obtained with 90% amplitude.

Although ultrasound is increasing the reaction rates, no major differences in eventual conversions were observed in comparison to the experiments in silent mode. Furthermore, the oxirane number seems to be decreasing by prolonging the reaction time, which indicates that the concentration of ring-opening products is increasing with time when applying ultrasound irradiation for intensifying the reaction process. Hence, the total reaction time should be shortened to 4-5 hours to minimize the concentrations of ring-opening products.

As previously mentioned, ultrasound irradiation promotes the formation of an emulsion between the organic and the aqueous phase, thus contributing to an efficient biphasic mass transfer. This was observed when withdrawing the samples, since a spontaneous phase separation was difficult to achieve without using a centrifuge. The observation of this phenomenon was diminished with time (Figure 11), which indicates that the emulsion is more stable when high amounts of unreacted fatty acid are present and not when epoxidized fatty acid is formed. This phenomenon caused unreliability issues in the analysis of the first samples of each experiment using ultrasound irradiation. Therefore, the iodine value, thus also the RCU value of the first sample, was corrected to the theoretical iodine value of oleic acid.

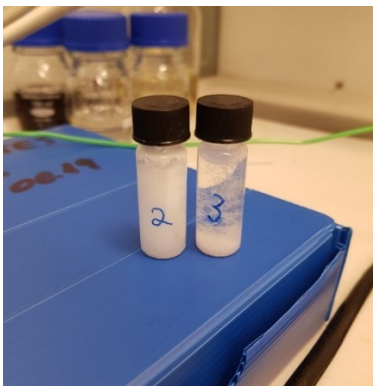

Figure 11 - Two sample bottles from an ultrasound experiment withdrawn after one and two hours of reaction time, accordingly

3.2.3. Influence of temperature

The reaction temperature for the sonochemical reactor was optimized by studying four different temperatures: 30 °C, 45 °C, 50 °C and 60 °C with a 1:2 fatty acid-to-hydrogen peroxide ratio using 90% ultrasound amplitude and 1000 rpm. Two of these experiments with lower temperatures (30 °C and 45 °C) were discontinued before the estimated reaction time of 8 hours due to product solidification on the glass walls of the reactor. This phenomenon caused severe mass transfer limitations (Figure 12), and it was likewise experienced in experiments performed with linoleic acid [10].

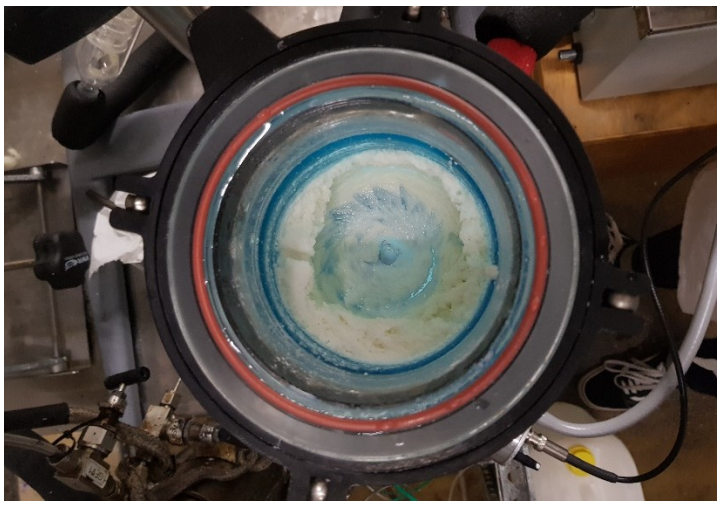

Figure 12 - An image of the solidification in the discontinued experiment at 30 °C. Picture taken from above of the batch reactor

Figure 13 shows that the best reaction conditions were found at 60 °C, where the highest RCO values of 86% were reached. Although 60 °C seems to be the optimal temperature, similar levels of RCO were reached at 50 °C and this temperature can be considered for preserving the enzymatic activity when the catalyst is being reused in several consecutive experiments [10], [27].

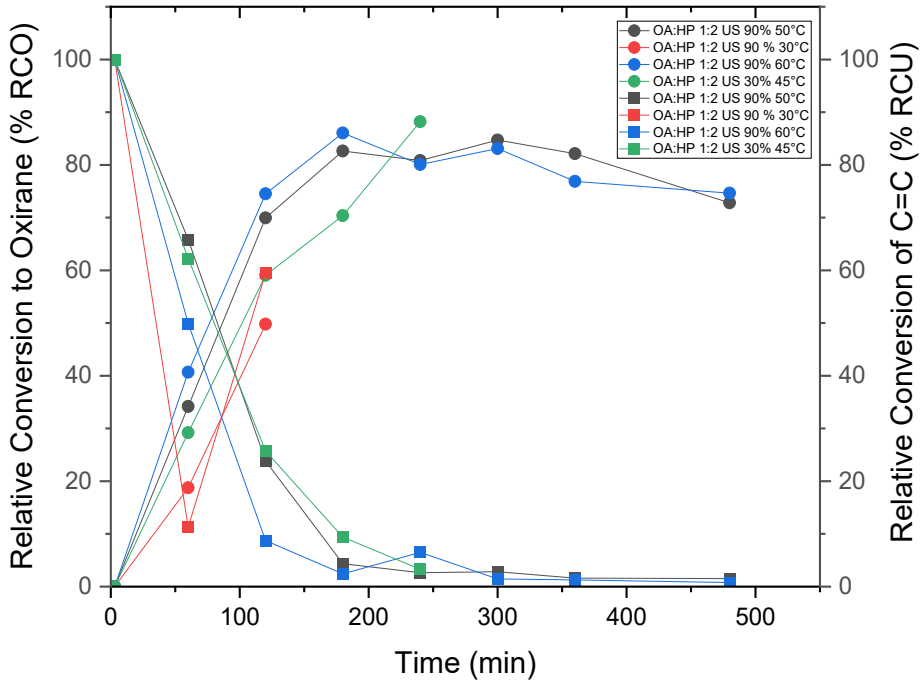

Figure 13 - Relative conversion of oxirane (RCO) and double bonds (RCU) for experiments in different temperatures with ultrasound

3.2.4. Influence of stirring speed

Stirring speed has an impact on the emulsion formation, hence on the mass transfer between the aqueous and organic phase. A stirring rate of 1000 rpm was chosen as the initial speed for the experiments, thus avoiding any mass transfer limitations that using the SpinChem® device could bring. Given the low efficiency of using SpinChem® for immobilizing the catalyst, a variation in stirring rate was implemented, since the device was only used as a stirrer with a centrifugal effect.

The stirring speed has to be high enough to create an emulsion and, accordingly, the stirring speeds were set to 500 rpm, 750 rpm and 1000 rpm in order to homogenize the liquid mixture well [19]. Previous studies have stated that a high stirring speed can result in a destruction of the immobilized lipase and, therefore, lower conversions in oxirane number have been obtained [11], [12]. As depicted in Figure 14 and, in contrary to the previous statements, a high stirring speed of 1000 rpm was appropriate for this system. One hypothesis is that the filter around the SpinChem® device is

protecting the immobilized lipase from being harmed by a grinding effect of the agitator (See schematic figure of SpinChem® RBR, Figure 3). However, even if high stirring rates were efficient, a lower speed seems to be more efficient for obtaining high values of conversion. A speed of 750 rpm is the most favorable one in terms of high conversions with a top RCO value of almost complete conversion. The results at 500 rpm and 1000 rpm led to comparably similar values in the reaction rate and conversion. As a conclusion, the reaction parameters of OA:HP ratio of 1:2, ultrasound amplitude of 90%, 60 °C and 750 rpm is the most favorable option of all the experiments conducted with a fresh catalyst.

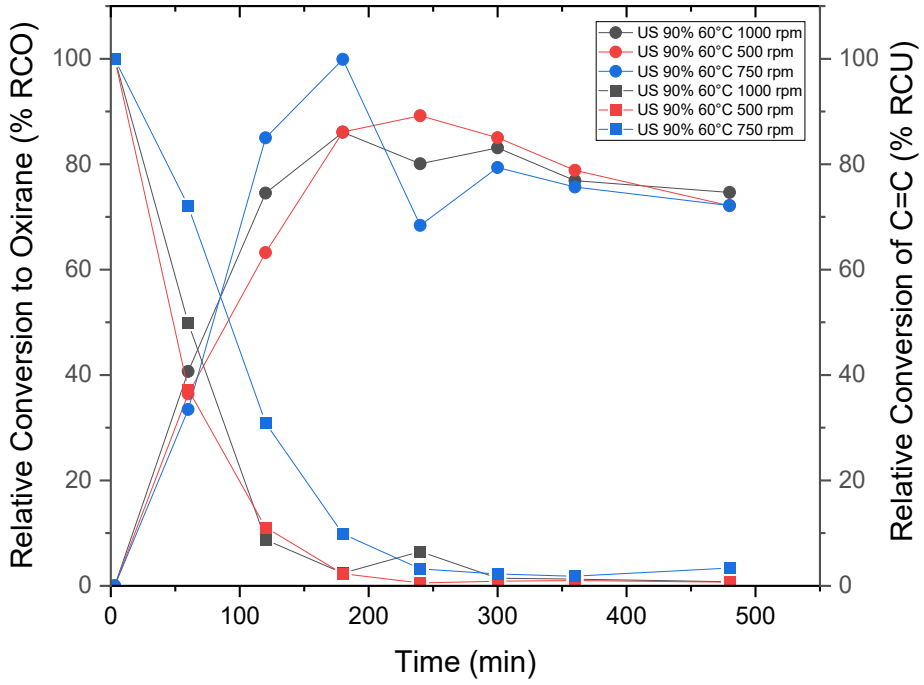

Figure 14 - Relative conversion of oxirane (RCO) and double bonds (RCU) for experiments using different stirring speeds with ultrasound

3.3. **Lipase reusability in conventional and sonochemical reactors**

The reusability of immobilized lipase is crucial for the economic viability of this process. The concept of catalyst recycling for this system was first practiced by Warwel and Rüsch gen. Klaas [16] using toluene as a solvent, continued by Orellana-Coca *et al*. [29] in a solvent-free medium, and by Bhalerao *et al*. [12] with toluene as the solvent, intensified by acoustic irradiation. The purpose of this work was to test the reusability in a solvent-free medium both in the absence and presence of ultrasound.

As previously mentioned, slightly lower amounts of hydrogen peroxide and a lower temperature were used in order to preserve the activity of the catalyst. Hence, the reaction conditions were set at 50 °C with a stirring speed of 750 rpm. The fatty acid-to-hydrogen peroxide molar ratios were set to 1:1.5 for experiments conducted in the absence of ultrasound, and to 1:1.75 for experiments in the presence of ultrasound. For a proper view on the ultrasound impact on the catalyst activity, the full power of 90% ultrasound amplitude was used. The catalyst was recovered after each experiment and reused in the next experiment. In order to reach equal levels of the catalyst load, new catalyst was added to the used one. The reusability levels for each experiment are described in Table 3.

Table 3 - Reaction parameters for the experiments studying lipase reusability in silent mode and with ultrasound

Reaction conditions	**Used catalyst (%)**
OA:HP 1:1.5 50 °C 750 rpm 1:st experiment	0
OA:HP 1:1.5 50 °C 750 rpm 2:nd experiment	59.3
OA:HP 1:1.5 50 °C 750 rpm 3:rd experiment	79.7
OA:HP 1:1.75 50 °C US 90% 750 rpm 1:st experiment	0
OA:HP 1:1.75 50 °C US 90% 750 rpm 2:nd experiment	67.8
OA:HP 1:1.75 50 °C US 90% 750 rpm 3:rd experiment	47.5

The experimental data in Figure 15 and Figure 16 show that, as an addition to the clear rate enhancing effect of ultrasound, the catalyst reusability is preserved for at least three consecutive experiments under the these reaction conditions. The ultrasound experiments reached almost full conversion to epoxides, while the silent experiments resulted in lower values of RCO.

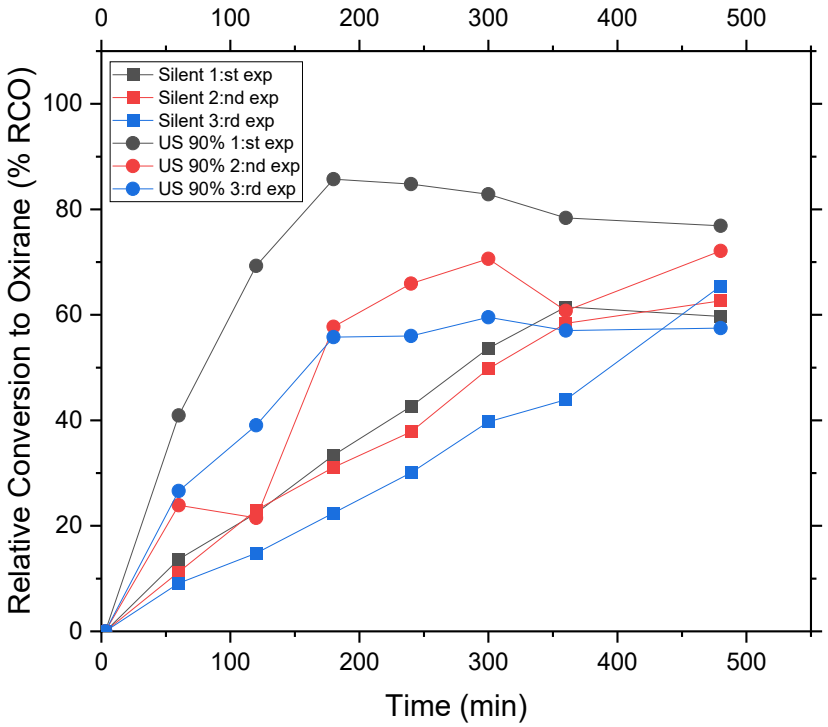

Figure 15 - Relative conversion to oxirane (RCO) for the reusability experiments in silent mode and ultrasound. The reaction conditions were OA:HP 1:1,5, 50 ºC and 750 rpm for silent experiments, and OA:HP 1:1,75, 50 ºC and 750 rpm for ultrasound experiments

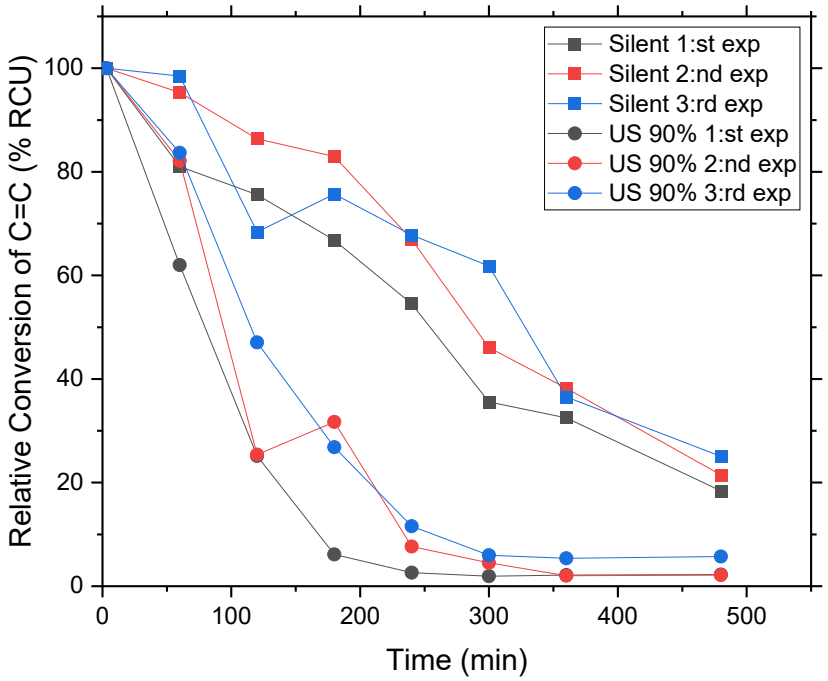

Figure 16 - Relative conversion of double bonds (RCU) for the reusability experiments in silent mode and with ultrasound. The reaction conditions were OA:HP 1:1,5, 50 ºC and 750 rpm for silent experiments, and OA:HP 1:1,75, 50 ºC and 750 rpm for ultrasound experiments

3.4. **Chemical composition of products – NMR analysis**

Nuclear Magnetic Resonance spectroscopy (NMR) was used to analyze the chemical composition of products obtained in silent mode, with ultrasound, and for the catalyst reusability experiments. The analyzed experiments were the molar ratio OA:HP 1:2 in silent mode and stirring at 1000 rpm (Table 2, experiment 8), OA:HP 1:2 with the ultrasound amplitude 90% and stirring at 500 rpm (Table 2, experiment 15) and OA:HP 1:1.75 with the ultrasound amplitude 90% using reused catalyst and with stirring at 750 rpm (Table 2, experiment 22). Two samples per each experiment, one after 4 hours and another one after 8 hours of reaction time, were analyzed. The complete ^{1}H spectra for all the analyzed samples can be found in Figure 17.

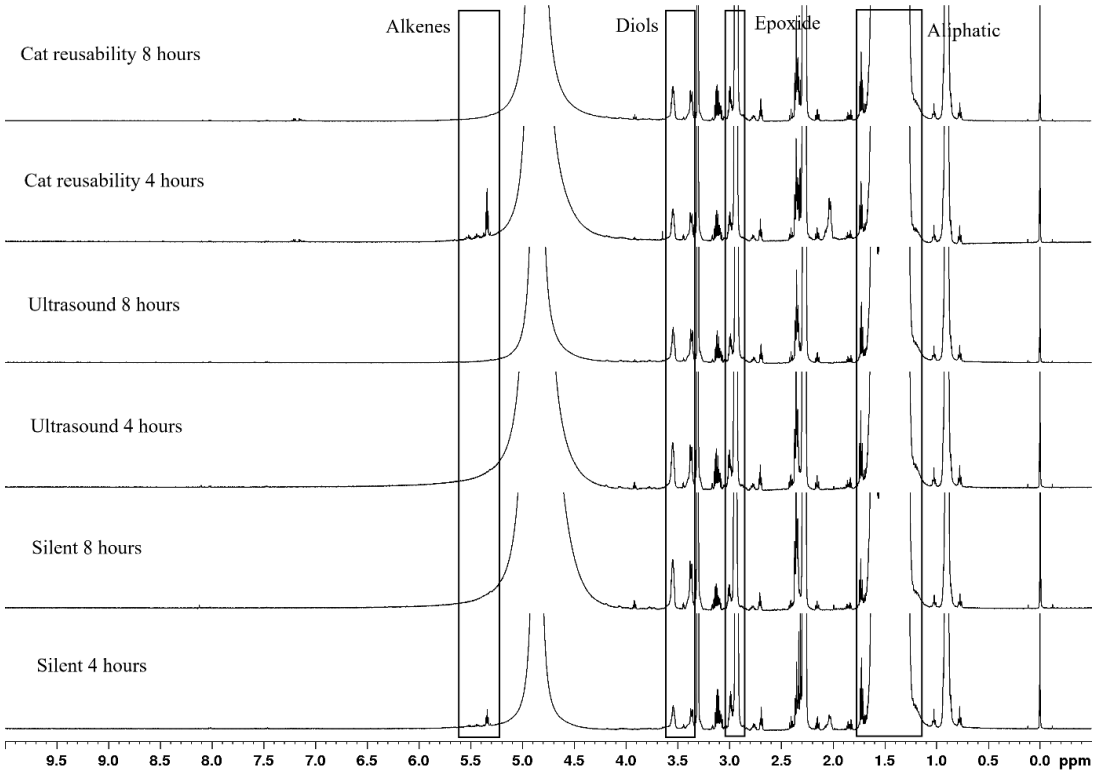

Figure 17 – NMR ^{1}H spectra with the characterized chemical shifts for all the analyzed samples

One major discovery from these spectra is that after four hours of reaction time, only for the experiment in silent mode and for the catalyst reusability experiment, some signs of unreacted double bonds from the fatty acid can be detected. After eight hours of reaction time, no remaining double bonds can be seen in the spectra. This implies that the conversion for all the experiments was complete.

Small amounts of ring-opening products in the form of diols and esters can be found in every analyzed sample, but larger peaks are found in the samples after 8 hours of reaction time. An analysis of the NMR spectra provides a result of ester-hydroxyls to diols ratio 1:0.4, thus, esters are the dominating ring-opening products. This means that the carboxylic groups are mainly the nucleophiles causing the ring-opening reactions, and not water. According to the NMR spectra, the largest amount of ring-opening products was found in the sample from the silent experiment, measuring about 10% of the products.

In the Prileschajew epoxidation, the system is operating in an acidic environment due to an addition of carboxylic acid, hence the probability for protonation of the oxirane ring is high. According to the provided spectra in Figure 17, a lower amount of ring-opening products was formed in this chemo-enzymatic epoxidation compared to a classical Prileschajew epoxidation [8]. The reason for this might be that lower amounts of possible nucleophiles is available in a system without carboxylic acid added, and only water and the carboxylic group in the fatty acid can be seen as nucleophiles leading to ring-opening of the epoxy group.

Minor peaks of a component consisting of a phenyl group attached by an alkyl chain is discovered from the experiment using reused catalyst and ultrasound. This is possibly caused by toluene that is used as a solvent for cleaning the catalyst before reuse. It is, however, a very small peak of approximately 0.07% of the whole sample concentration. It could be interesting to further study the impact of combining reused catalyst and ultrasound irradiation by reusing the catalyst in several consecutive experiments.

3.5. **Catalyst durability – SEM analysis**

The morphology of the immobilized lipase was studied with Scanning Electron Microscopy (SEM). Fresh catalyst as well as reused catalyst originating from experiments both in silent mode and ultrasound were studied. The SEM images from a fresh catalyst (Figure 18) and a catalyst used in silent mode (Figure 19) show that the shape of Novozym® 435 is preserved well during the experiments conducted in silent mode. However, the catalyst lost its beauty after three consecutive uses with ultrasound due to the cavitation phenomena, impacting the catalyst surface (Figure 20). It is remarkable that the catalyst is keeping its activity despite the destruction of the catalyst shape. One hypothesis for the good preservation of the activity is that the catalyst surface area increases as a result of the destruction of the surface, hence enabling an easier access to the available active sites. For getting a better understanding about the catalyst performance, further analysis with a nitrogen adsorption analyzing method could be performed. This would give one a more precise understanding on the changes in the specific area of the catalyst. A complete set of SEM images from all reusability experiments can be found in Appendix II.

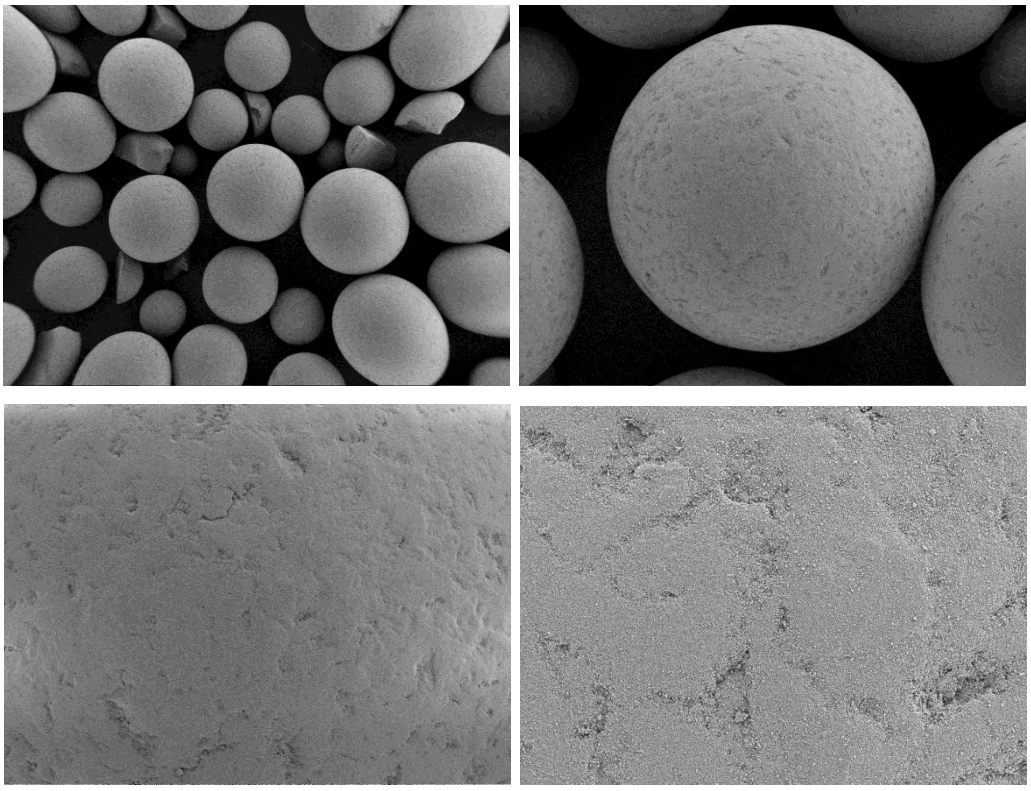

Figure 18 - SEM images (30x, 100x, 250x and 1000x size from left to right, accordingly) of unused immobilized lipase

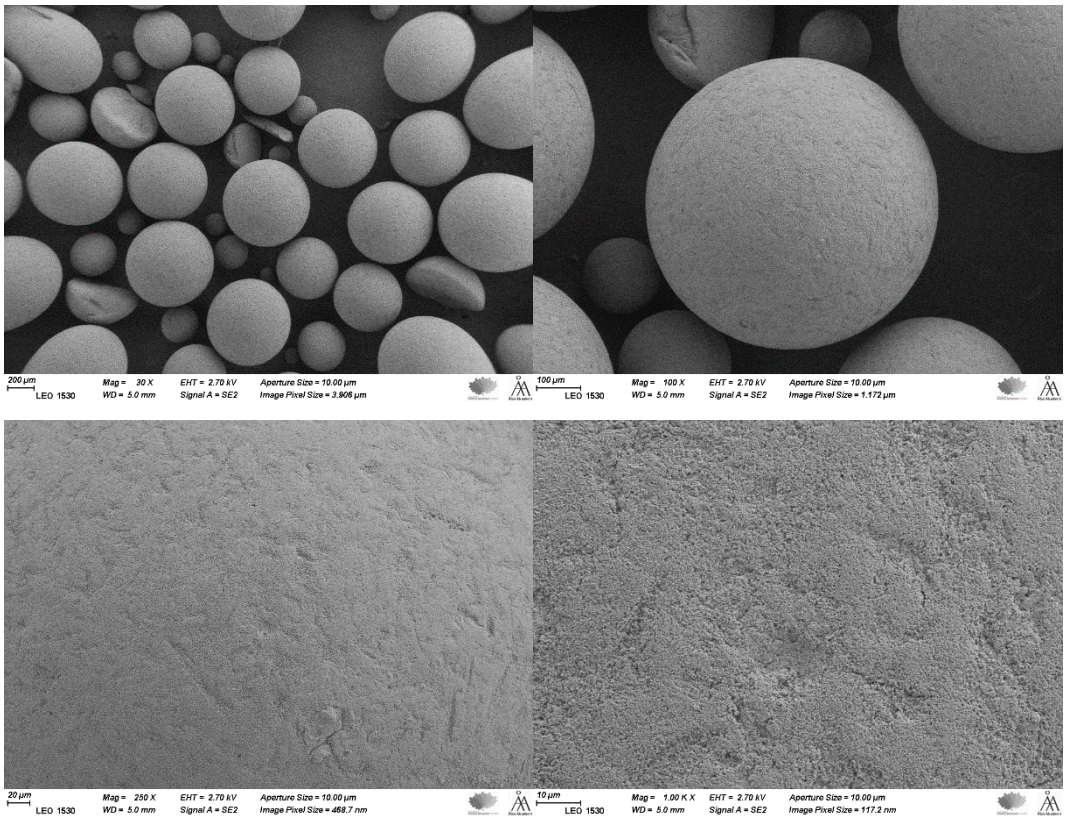

Figure 19 - SEM images (30x, 100x, 250x, and 1000x size from left to right, accordingly) of immobilized lipase after three consecutive uses in silent mode

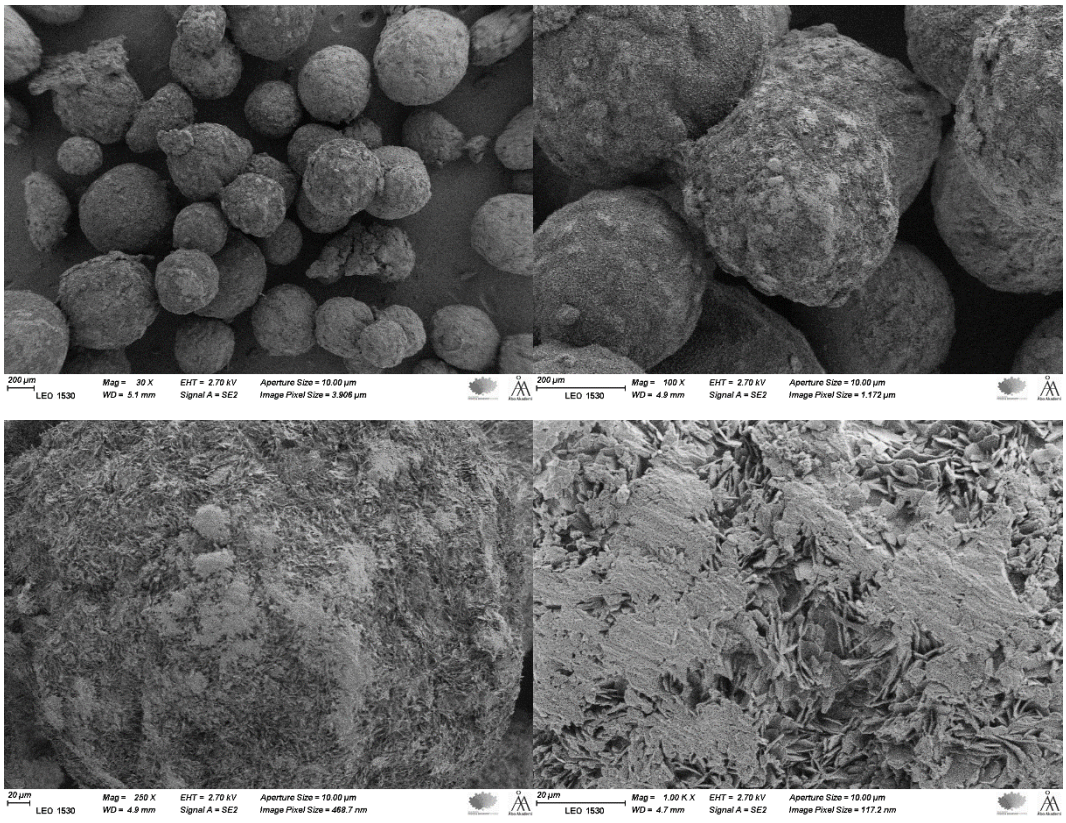

Figure 20 - SEM images (30x, 100x, 250x, and 1000x size from left to right, accordingly) of immobilized lipase after three consecutive uses with ultrasound irradiation

3.6. **Kinetic modelling**

3.6.1. Reaction stoichiometry

A kinetic model for the chemo-enzymatic self-epoxidation of fatty acids has earlier been presented by Yadav *et al.* [26], which can be considered as a simplified version of the reaction mechanism proposed by Warvel *et al*. [25]. The model by Yadav *et al.* assumes that the formation of peroleic acid after the perhydrolysis process is briefly lasting, hence there is no accumulation of peroleic acid in the system. Therefore, an assumption of direct epoxidation between oleic acid and hydrogen peroxide catalyzed by lipase has been made in one of the proposed kinetic models in this work. The molecular mechanism proposed by Warvel *et al.* makes no such assumption and, therefore, the formation of peroleic acid is an aspect that has as well been taken into consideration. The molecules considered in this work are represented in Figure 21.

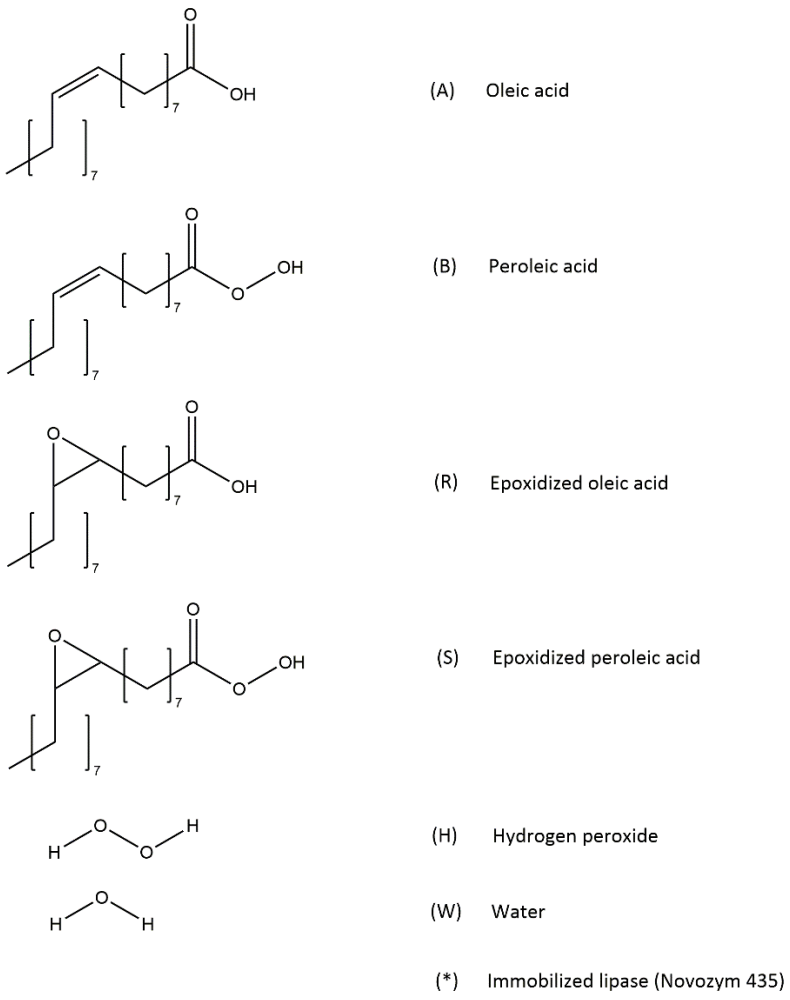

Figure 21 – Molecules in the reaction mechanisms

Two different hypotheses of the rate determining stoichiometric steps have been formed, one with peroleic acid and one without it.

Alternative 1:

$$A + H \rightarrow B + W \quad \text{(I)}$$

$$B + A \rightarrow R + A \quad \text{(II)}$$

$$B + B \rightarrow S + A \quad \text{(III)}$$

The second alternative for the stoichiometry is assuming a direct epoxidation of oleic acid (A) and hydrogen peroxide (H) and, thus, no peroleic acid (B) is formed. Consequently, no epoxidized peroleic acid (S) is formed in this version.

Alternative 2:

$$A + H \rightarrow R + W \quad \text{(IV)}$$

Both options for the stoichiometry can be extended to obtain a better overview on the reaction steps. A typical way to do this is by dividing the steps into adsorption, bimolecular surface reactions, and desorption steps. Here, the catalyst surface site (*) is included in the mechanisms.

3.6.2. Epoxidation mechanisms and rate equations

Different options for the epoxidation mechanisms should be considered in the modelling work. Four different competing models are described and evaluated, using the previously described alternatives for the overall stoichiometry.

Model 1

In this model, the concept of using the Langmuir-Hinshelwood mechanism in heterogeneous catalysis is used. Here all the molecules adsorbed on the catalyst surface react, eventually creating the product. The assumption that all components are adsorbed only to one active catalyst site each is used. These assumptions give the following detailed mechanism:

Table 4 - The reaction steps in model 1

	Reaction steps
Adsorption	$A + * \rightleftharpoons A*$ $B + * \rightleftharpoons B*$ $\mathrm{H} + * \rightleftharpoons \mathrm{H}*$ $\mathrm{W}* \rightleftharpoons \mathrm{W} + *$
Bimolecular reactions (Surface reaction)	$A* + H* \rightarrow B* + W*$ *(I)* $A* + B* \rightarrow R* + A*$ *(II)* $B* + B* \rightarrow S* + A*$ *(III)*
Desorption	$R* \rightleftharpoons R + *$ $S* \rightleftharpoons S + *$

The overall reactions result in

$A + H \rightarrow B + W$ (I)

$B + A \rightarrow R + A$ (II)

$B + B \rightarrow S + A$ (III)

In this model, the adsorption and desorption steps can be interpreted as rapid reactions reaching quasi-equilibria, being rapid compared to the time-demanding and irreversible bimolecular steps. The generation rates r_I, r_{II} and r_{III} for the overall reaction steps can be described as

$$r_I = k_I c_A * c_H * \quad (6)$$

$$r_{II} = k_{II} c_A * c_B * \quad (7)$$

$$r_{III} = k_{III} c_B *^2 \quad (8)$$

The equilibrium constant of the adsorption and desorption quasi-equilibria steps can be expressed as

$$K_i = \frac{c_i *}{c_i c *} \quad (9)$$

and this expression can be rearranged to

$$c_i^* = K_i c_i c^* \quad (10)$$

where c_i* represents the concentrations for all molecules adsorbed on an active catalyst site. Adding the concentration of vacant surface sites $c*$ brings us to a total concentration of catalyst surface sites c_0,

$$c * + \sum c_j * = c_0 \quad (11)$$

Thus, the following equations can be used for calculating the concentration of vacant sites $c*$ and for the concentration of adsorbed molecules on catalyst c_j*, respectively

$$c* = \frac{c_0}{1 + \sum K_j c_j} \quad (12)$$

$$c_i * = \frac{K_i c_i c_0}{1 + \sum K_j c_j} \quad (13)$$

Inserting these into the rate equations (6)-(8) gives the following rate equations

$$r_I = \frac{k_I K_A K_H c_A c_H c_0^{\,2}}{(1+\sum K_j c_j)^2} \tag{14}$$

$$r_{II} = \frac{k_{II} K_A K_B c_A c_B c_0^{\,2}}{(1+\sum K_j c_j)^2} \tag{15}$$

$$r_{III} = \frac{k_{III} K_B^{\,2} c_B^{\,2} c_0^{\,2}}{(1+\sum K_j c_j)^2} \tag{16}$$

The adsorption equilibrium constants K_i and the rate constants k_i are merged to a constant k'_i, hence the following compact forms of the rate expressions can be used,

$$r_I = \frac{k'_1 c_A c_H c_0^{\,2}}{(1+\sum K_j c_j)^2} \tag{17}$$

$$r_{II} = \frac{k'_2 c_A c_B c_0^{\,2}}{(1+\sum K_j c_j)^2} \tag{18}$$

$$r_{III} = \frac{k'_3 c_B^{\,2} c_0^{\,2}}{(1+\sum K_j c_j)^2} \tag{19}$$

where

$$\sum K_j c_j = K_A c_A + K_B c_B + K_R c_R + K_S c_S + K_H c_H + K_W c_W \tag{20}$$

for j = A, B, R, S and H. An assumption of significantly lower equilibrium constants of R, S, B, H, and W compared to A leads us to a useful approximation

$$\sum K_j c_j = K_A c_A \tag{21}$$

In previous sections, the existence of ring-opening products were proven by the titriometrically obtained results, and later confirmed by the NMR analysis. In order to obtain a realistic description of the reaction kinetics and to improve the model fit to experimental data, the rate of ring-opening has to be included in the model. Bimolecular reactions were assumed for the ring-opening reactions.

$$r_{ROPi} = -k_{ROP} c_A c_i \tag{22}$$

for i= R and S.

The component generation rates are then calculated by

$$r_A = -r_I + r_{III} - r_{ROPR} - r_{ROPS} \quad (23)$$

$$r_B = r_I - r_{II} - 2r_{III} \quad (24)$$

$$r_R = r_{II} - r_{ROPR} \quad (25)$$

$$r_S = r_{III} - r_{ROPS} \quad (26)$$

$$r_H = -r_I \quad (27)$$

$$r_W = r_I \quad (28)$$

Model 2

The underlying theory behind this model is based on the assumption that no peroleic acid is accumulated, as presented previously by Yadav *et al.* [26]. Here an active complex is formed between oleic acid (A), hydrogen peroxide (H) and the immobilized lipase (*). The adsorption of water (W) and hydrogen peroxide (H) was neglected. All reaction steps are presented in .

Table 5 - The reaction steps in model 2

	Reaction steps
Adsorption	$A + * \rightleftharpoons A*$
Bimolecular reactions	$A* + H \rightarrow AH*$
(Active complex)	$AH* \rightarrow R* + W$
Desorption	$R* \rightleftharpoons R + *$

Here the overall reaction is

$$A + H \rightleftharpoons R + W \quad \text{(IV)}$$

The step where the active complex is reacting is regarded as the rate-determining step, thus the other steps can be seen as rapid ones in the comparison. Therefore, the rate expression becomes

$$r = kc_{AH}* \quad (29)$$

The equilibria of the adsorbed molecules are defined as

$$K_A = \frac{c_A *}{c_A c *} \tag{30}$$

$$K_R = \frac{c_R *}{c_R c *} \tag{31}$$

$$K_{AH} = \frac{c_{AH} *}{c_A * c_H} \tag{32}$$

and the total concentration on the catalyst surface can be expressed by

$$c_A * + c_{AH} * + c_R * + c * = c_0 \tag{33}$$

By using the expressions for calculating the vacant surface sites and the total concentration of the absorbed molecules on catalyst surface, the following rate expression is formed,

$$r = \frac{k K_A K_{AH} c_A c_H c_0}{1 + K_A c_A + K_A K_{AH} c_A c_H + K_R c_R} \tag{34}$$

with the compact version formed similarly as in Model 1

$$r = \frac{k' c_A c_H c_0}{1 + K_A c_A + K_A K'_{AH} c_A c_H + K_R c_R} \tag{35}$$

The component generation rates, including the rates of ring-opening are

$$r_A = -r - r_{ROPR} \tag{36}$$

$$r_R = r - r_{ROPR} \tag{37}$$

$$r_H = -r \tag{38}$$

$$r_W = r \tag{39}$$

where the rate for ring-opening is obtained from

$$r_{ROPi} = -k c_A c_i \tag{40}$$

for i= R

Model 3

This model is a combination of the two previously presented models. Here the theory relies on the hypothesis that peroleic acid (B) is formed through a reaction of an active complex between oleic acid (A), hydrogen peroxide (H) and lipase (*). This peroleic acid (B) reacts further with oleic acid (A) and peroleic acid (B), creating epoxidized oleic acid and epoxidized peroleic acid. The mechanism of this model is presented in

.

Table 6 - The reaction steps in model 3

	Reaction steps
Adsorption	$A + * \rightleftharpoons A*$
Bimolecular reactions and active complex	$A* + H \rightleftharpoons AH*$ $AH* \rightarrow B* + W$ $A* + B* \rightarrow R* + A*$ $B* + B* \rightarrow S* + A*$
Desorption	$B* \rightleftharpoons B + *$ $R* \rightleftharpoons R + *$ $S* \rightleftharpoons S + *$

The overall reactions for the rate determining steps are analogously

$A + H \rightarrow B + W$ (I)

$B + A \rightarrow R + A$ (II)

$B + B \rightarrow S + A$ (III)

the rate equations being

$r_I = k_I c_{AH}*$ (41)

$r_{II} = k_{II} c_A * c_B *$ (42)

$r_{III} = k_{III} c_B *^2$ (43)

while the equilibrium constant of the adsorbed molecules *i*= A, B, R and S is

$$K_i = \frac{c_i *}{c_i c*} \tag{44}$$

and equally for the complex AH*

$$K_{AH} = \frac{c_{AH} *}{c_H c_A *} \tag{45}$$

The total balance of concentration on catalyst surface is expressed by

$$c_A * + c_{AH} * + c_B * + c_R * + c_S * + c* = c_0 \tag{46}$$

The concentration of vacant catalyst sites can be expressed by the following equation,

$$c* = \frac{c_0}{1 + \sum K_j c_j + K_A K_{AH} c_A c_H} \tag{47}$$

finally resulting in the compressed forms of rate equations for the rate determining reactions

$$r_1 = \frac{k'_1 c_A c_H c_0}{1 + \sum K_j c_j + K c_A c_H} \tag{48}$$

$$r_2 = \frac{k'_2 c_A c_B c_0^{\,2}}{(1 + \sum K_j c_j + K c_A c_H)^2} \tag{49}$$

$$r_3 = \frac{k'_3 c_B^{\,2} c_0^{\,2}}{(1 + \sum K_j c_j + K c_A c_H)^2} \tag{50}$$

and the denominator comprises the following expressions

$$\sum K_j c_j = K_A c_A + K_B c_B + K_R c_R \tag{51}$$

and

$$K = K_A K_{AH} \tag{52}$$

The component generation rates can be calculated from

$$r_A = -r_I + r_{III} - r_{ROPR} - r_{ROPS} \quad (53)$$

$$r_B = r_I - r_{II} - 2r_{III} \quad (54)$$

$$r_R = r_{II} - r_{ROPR} \quad (55)$$

$$r_S = r_{III} - r_{ROPS} \quad (56)$$

$$r_H = -r_I \quad (57)$$

$$r_W = r_I \quad (58)$$

The rate for ring-opening r_{ROPi} is obtained analogously as in model 1.

Model 4

An assumption of the adsorption of oleic acid (A) and hydrogen peroxide (H) on the catalyst surface (*) is applied in this model. The product (R) is formed through an active complex that is formed on the catalyst surface, hence no peroleic acid (B) is formed. The hypothetical mechanism comprises the following steps listed in Table 7.

Table 7 - The reaction steps in model 4

	Reaction steps
Adsorption	$A + * \rightleftharpoons A*$ $H + * \rightleftharpoons H*$
Bimolecular reaction	$A* + H* \rightarrow R* + W*$
Desorption	$R* \rightleftharpoons R + *$ $W* \rightleftharpoons W + *$

The overall reaction is

$$A + H \rightarrow R + W \quad (59)$$

The rate expression is defined by

$$r = kc_A * c_H * \quad (60)$$

and the total balance for the adsorbed components is

$$c_A{}^* + c_H{}^* + c_R{}^* + c_W{}^* + c^* = c_0 \tag{61}$$

leading to the compressed form of the rate equation,

$$r = \frac{k' c_A c_H c_0{}^2}{(1 + \sum K_j c_j)^2} \tag{62}$$

where the term in the denominator is defined by the following terms,

$$\sum K_j c_j = K_A c_A + K_H c_H + K_R c_R + K_W c_W \tag{63}$$

Assuming that the adsorption of hydrogen peroxide, epoxide and water is low, an optimized expression would be,

$$\sum K_j c_j = K_A c_A \tag{64}$$

The rate equations for components are,

$$r_A = -r - r_{ROPR} \tag{65}$$

$$r_R = r - r_{ROPR} \tag{66}$$

$$r_H = -r \tag{67}$$

$$r_W = r \tag{68}$$

The rate equation for the ring-opening r_{ROPR} is obtained analogously as in model 2.

3.6.3. Component mass balances

As previously mentioned, the interfacial mass transfer between the aqueous and the organic phase is one of the key steps for this liquid-liquid-solid system. It can be assumed that the actual epoxidation reaction takes place in the organic phase, while the formation of peroleic acid through perhydrolysis takes place in the aqueous phase [44]. Therefore, the mass balances are divided into two parts according to the reaction phase.

The mass balance of hydrogen peroxide and water in the aqueous phase is described as

$$0 = N_i A + \frac{dn_{ai}}{dt} \tag{69}$$

for i= H, W. Analogously, the expression for the organic phase mass transfer

$$N_i A + r_i m_{cat} = \frac{dn_{oi}}{dt} \tag{70}$$

where A is the interfacial area between the aqueous and organic phases and m_{cat} is the mass of the catalyst. By assuming that the interfacial mass transfer is rapid compared to the reactions in both phases, these two phase-dependent mass transfer differential equations can be combined to,

$$r_i m_{cat} = \frac{dn_{ai}}{dt} + \frac{dn_{oi}}{dt} \tag{71}$$

The change in volume in both phases is assumed to be negligible. Hence, the phase-specific mass balances can be expressed as follows,

$$\frac{dn_{ai}}{dt} = V_a \frac{dc_{ai}}{dt} \tag{72}$$

$$\frac{dn_{oi}}{dt} = V_o \frac{dc_{oi}}{dt} \tag{73}$$

Consequently, a total mass balance can be written as

$$V_a \frac{dc_{ai}}{dt} + V_o \frac{dc_{oi}}{K_i dt} = r_i m_{cat} \tag{74}$$

where K_{Di} is the distribution coefficient of a component i = H, W between the phases, defined by

$$K_{Di} = \frac{c_{ai}}{c_{oi}} \tag{75}$$

For this liquid-liquid-catalyst three phase reactor, the catalyst bulk density is defined as

$$\rho_c = \frac{m_{cat}}{V_0} \tag{76}$$

This is introduced into the mass balance (74), finally resulting in

$$\frac{dc_{ai}}{dt} = \frac{r_i \rho_c}{V_a / V_o + 1 / K_i} \tag{77}$$

Additionally, the ratio for volume distribution between phases is introduced,

$$\alpha = \frac{V_a}{V_a + V_o} = \frac{V_a / V_0}{V_a / V_0 + 1} \tag{78}$$

$$\frac{V_a}{V_o} = \frac{\alpha}{1-\alpha} \tag{79}$$

Inserting this expression in equation (77), it leads us to

$$\frac{dc_{ai}}{dt} = \frac{(1-\alpha) r_i \rho_c}{\alpha + (1-\alpha) / K_i} \tag{80}$$

An analogous approach can be used for the organic phase concentration,

$$\frac{dc_{oi}}{dt} = \frac{(1-\alpha) r_i \rho_c}{\alpha K_i + 1 - \alpha} \tag{81}$$

Equations (80) and (81) are created for components that exist in both phases (*i*= H, W), while the components that only exist in the organic phase (*i*= A, B, R and S) follow the model,

$$\frac{dc_{oi}}{dt} = r_i \rho_c \tag{82}$$

By this, we have a complete series of differential equations for the reactor modelling.

3.6.4. Parameter estimation

The parameter estimation for the mathematical model is based on the titrimetric analysis results consisting of the following parts: oxirane number for determining the amount of epoxy groups, iodine value for the remaining, unreacted double bonds, and hydrogen peroxide concentration. The analysis results, which are previously presented and discussed in this work, are divided into three different states for optimizing the reaction parameters as shown below.

Organic phase:

$$s_1 = c_A + c_B \tag{83}$$

$$s_2 = c_R + c_S \tag{84}$$

Aqueous phase:

$$s_3 = c_{aH} \tag{85}$$

The parameter estimation is executed by minimizing the objective function Q, consisting of the sum of squares between the experimental data $s_{i,exp}$ and the estimated values s_{it},

$$Q = \sum \sum (s_{i,t\,\exp} - s_{it})^2 \tag{86}$$

In order to reach optimal parameters for fitting the model to experimental data, a series of repeated parameter estimations was carried out using the function *lsqcurvefit* with a Levenberg-Marquardt algorithm [45] in the MATLAB 2019b software. The parameter estimation was performed simultaneously while using the function *ode45*, which is implementing the 4th order Runge-Kutta method for a numerical solution of systems of ordinary differential equations [46], [47].

The estimated unknown parameters in models 1 and 3 were the rate constants k'_1 and k'_2, and k_{ROP}, the adsorption equilibrium constants K_A and K_H, and the distribution coefficient K_{DH}. The rate constant k'_3 for the rate equation r_3 was neglected due to parameter values close to zero. In model 2, the rate constants k' and k_{ROP}, the adsorption equilibrium constants K_A, K_{AH}, and the distribution coefficient K_{Di} were

estimated. Model 4 was optimized to a four-parameter model, implying that only k', k_{ROP}, K_A and K_{DH} were estimated. The adsorption equilibrium constants K_B, K_R, K_W, and K_S were not considered in any parameter estimations due to a predominant adsorption of A over the rest of the components. Detected outliers in the experimental data were corrected by interpolation for reaching a better fit of the computed data by the model. Table 8 show the estimated parameters and the statistical errors and results for the estimations.

Table 8 - Estimated rate and equilibrium constants for Model 1

	Parameter	Std. Error	Relative Std. Error (%)	Parameter/Std. Error
k'_1	0.105E-01	0.310E-02	29.9	3.3
k'_2	0.259E-01	0.790E-02	30.3	3.3
k_{ROP}	0.607E-03	0.659E-03	108.5	0.9
K_A	0.362E00	0.120E00	33.2	3.0
K_{DH}	0.654E00	0.100E00	15.3	6.5

Table 9 - Estimated rate and equilibrium constants for Model 2

	Parameter	Std. Error	Relative Std. Error (%)	Parameter/Std. Error
k'	0.418E-01	0.493E-01	117.8	0.8
k_{ROP}	0.100E-02	0.172E-03	17.0	5.9
K_A	0.587E+01	0.771E+01	131.4	0.8
K_{AH}	0.138E00	0.146E00	105.8	0.9
K_{DH}	0.471E00	0.550E-01	11.7	8.6

Table 10 - Estimated rate and equilibrium constants for Model 3

	Parameter	Std. Error	Relative Std. Error (%)	Parameter/Std. Error
k'_1	0.119E-01	0.660E-02	55.5	1.8
k'_2	0.400E+04	0.610E+04	152.6	0.7
k_{ROP}	0.276E-04	0.434E-05	15.7	6.4
K_A	0.787E00	0.581E00	73.9	1.4
K_{DH}	0.335E00	0.522E-01	15.6	6.4

Table 11 Estimated rate and equilibrium constants for Model 4

	Parameter	Std. Error	Relative Std. Error (%)	Parameter/Std. Error
k'	0.160E-01	0.580E-02	36.4	2.7
k_{ROP}	0.100E-02	0.181E-03	17.8	5.6
K_A	0.692E00	0.223E00	32.2	3.1
K_{DH}	0.476E00	0.557E-01	11.7	8.5

Table 12 - Statistical results for the models

	Residual sum of squares
Model 1	9.36
Model 2	8.32
Model 3	8.32
Model 4	8.48

The best model is determined by comparing the accuracy of estimated parameters (Table 8-Table 11) and the estimated fit to the experimental data (Figure 22-Figure 25). Model 4 shows the best parameter estimation for the reproduction of the experimental data with relative standard errors below 40% for all estimated parameters. However, considering the low concentrations of the ring-opening products that are formed in the reaction, Model 1 shows nearly as good signs of accuracy as Model 4, despite a broad confidence interval for k_{ROP}. When taking the molecular aspects into consideration, it is likely that the formation of peroleic acid is needed for a spontaneous epoxidation reaction, as in the case for the Prileschajew epoxidation. Thus, models 1 and 3 are the most probable mechanisms for this chemo-enzymatic epoxidation, model 1 being the most accurate one.

The statistical results in Table 12 show, however, that the difference in the residual sum of squares between all four competing models is very small, thus, the fit of all models can be considered similar. Another observation is that the perhydrolysis step r_I seems to be remarkably slower than the epoxidation step r_{II}. Thus, it can be concluded that the perhydrolysis step is rate determining in this chemo-enzymatic epoxidation of fatty acids. This observation is analogous with previous studies of the classical Prileschajew epoxidation method [22], [48].

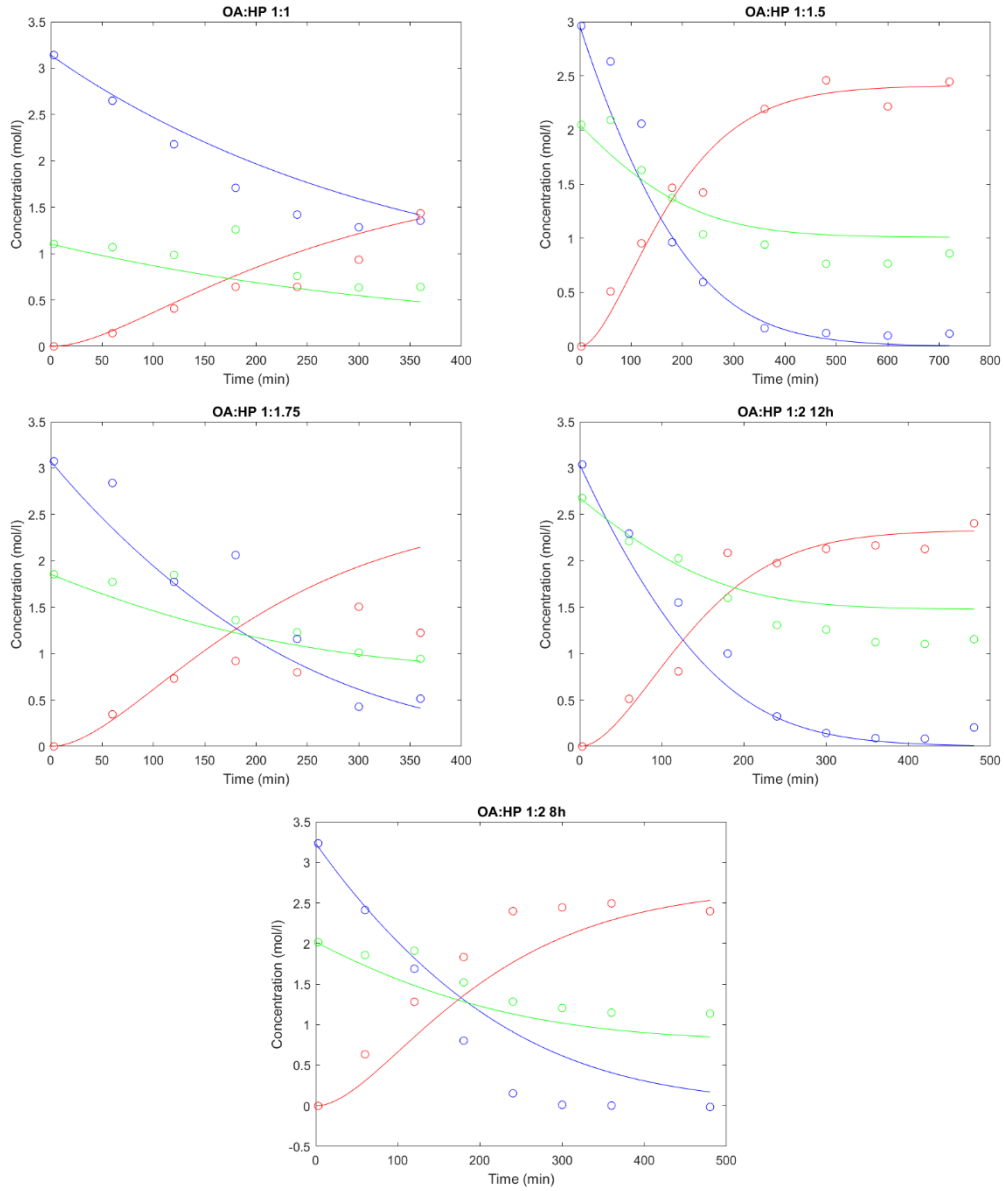

Figure 22 - Model 1 fitted to experimental data with OA:HP ratios of 1:1, 1:1.5, 1.75, and 1:2 in 50 C, stirring 1000 rpm conducted in silent mode. Lines: computed values, circles: experimental data. Blue: Oleic acid, Green: Hydrogen peroxide, Red: Epoxide

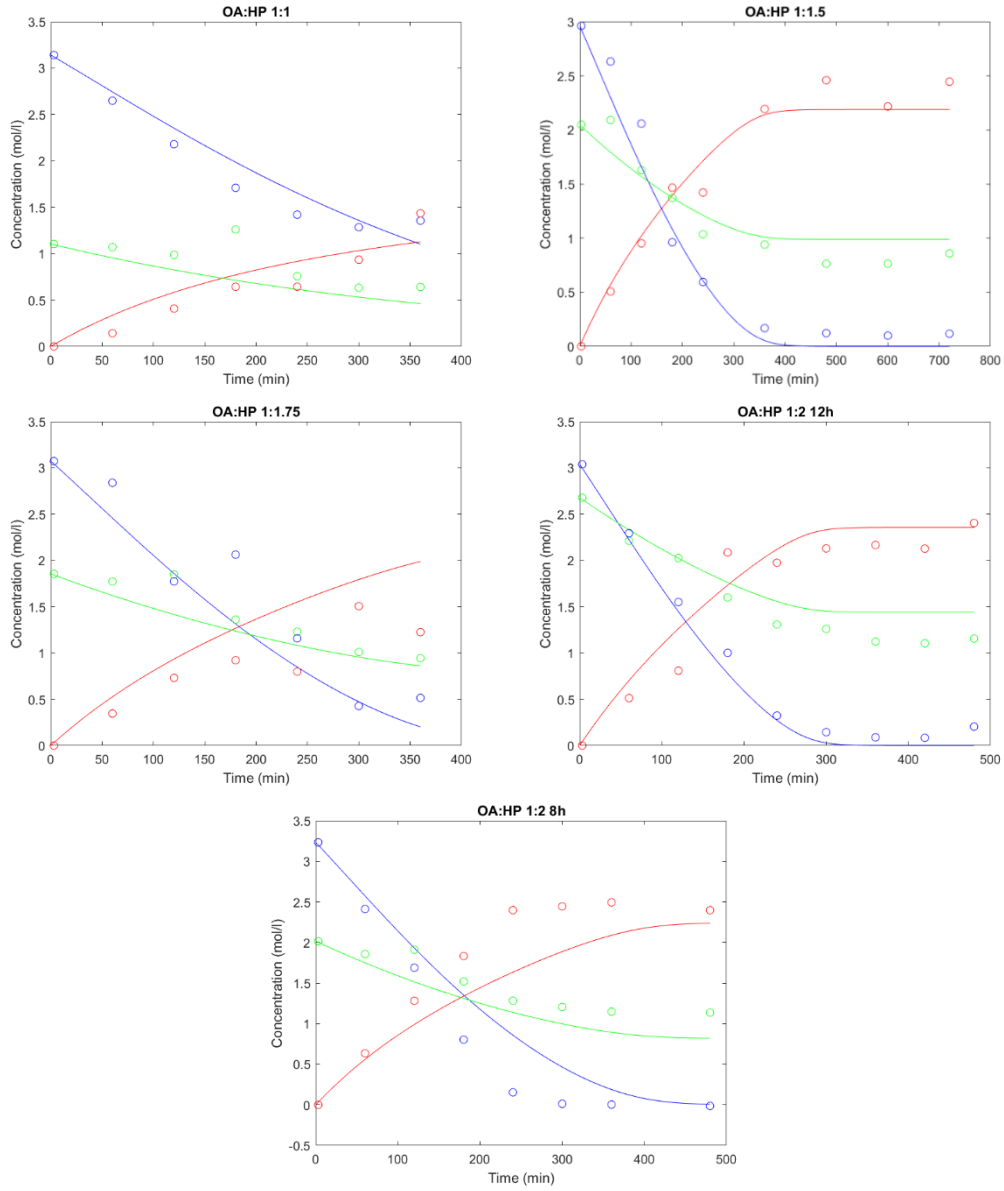

Figure 23 - Model 2 fitted to experimental data with OA:HP ratios of 1:1, 1.5, 1.75, and 1:2 in 50 C, stirring 1000 rpm conducted in silent mode. Lines: computed values, circles: experimental data. Blue: Oleic acid, Green: Hydrogen peroxide, Red: Epoxide

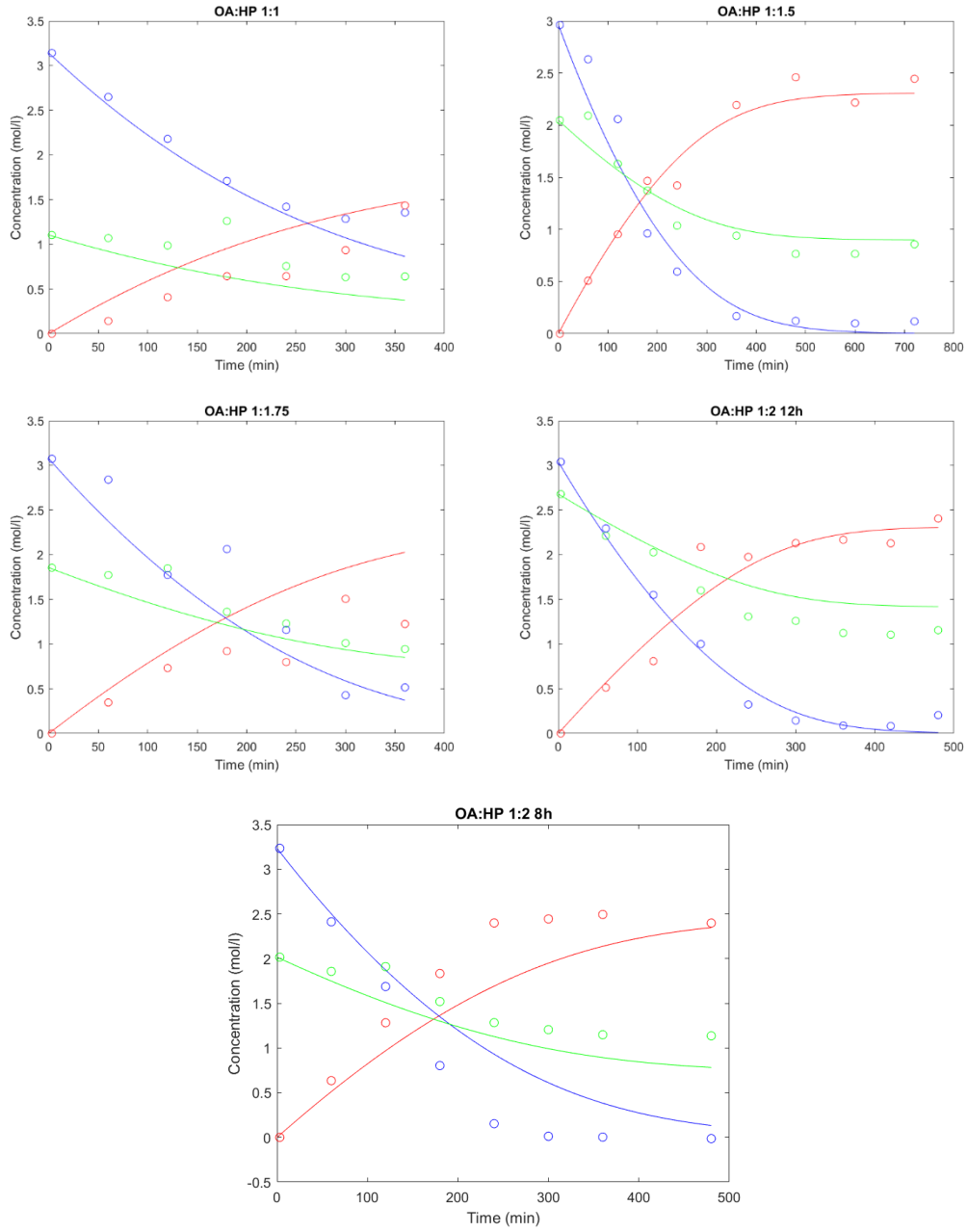

Figure 24 - Model 3 fitted to experimental data with OA:HP ratios of 1:1, 1:1.5. 1.75, and 1:2 in 50 C, stirring 1000 rpm conducted in silent mode. Lines: computed values, circles: experimental data. Blue: Oleic acid, Green: Hydrogen peroxide, Red: Epoxide

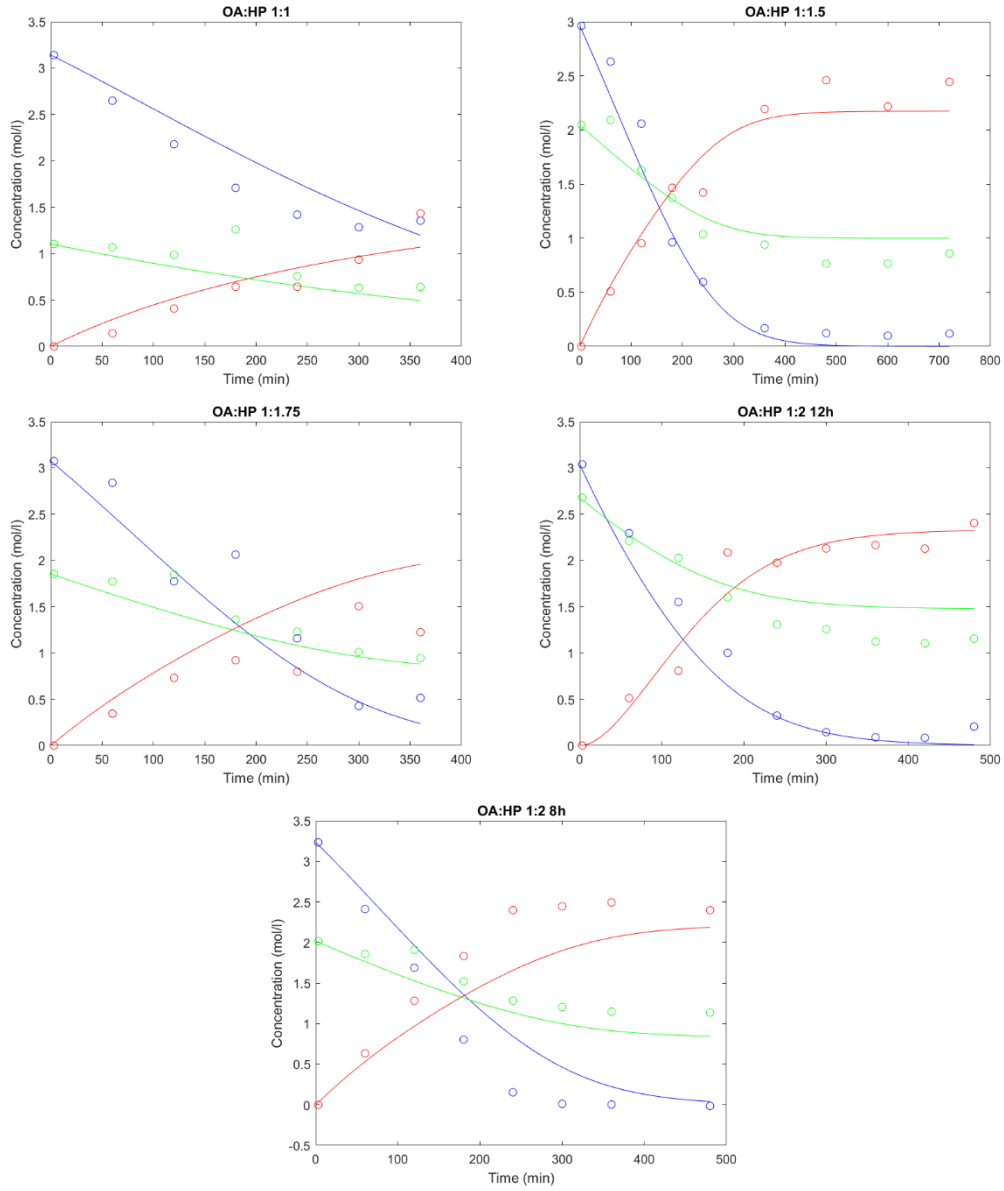

Figure 25 - Model 4 fitted to experimental data with OA:HP ratios of 1:1, 1:1.5. 1.75, and 1:2 in 50 C, stirring 1000 rpm conducted in silent mode. Lines: computed values, circles: experimental data. Blue: Oleic acid, Green: Hydrogen peroxide, Red: Epoxide

4. Conclusions

Epoxidation of oleic acid with the enzymatic approach using immobilized lipase as catalyst was successfully performed in this work. The results of the experiments showed that very high conversions of the double bonds in oleic acid are achievable by this method.

The original plan was to conduct the experiments using the SpinChem® RBR as a rotating catalyst bed, yet the conversions did not reach feasible levels. This was possibly caused by the high viscosity of oleic acid that impaired the mass transfer from the liquid to the catalyst. However, using the same device as a stirrer delivered promising results, thus leading to a conclusion that using SpinChem as an empty stirring device is sufficient for this purpose.

The concentrations of hydrogen peroxide has an impact on the conversions, particularly in silent systems where an OA:HP molar ratio of 1:2 provided the highest reaction rates, but also 1:1.5 reached similar conversion levels on a longer 12-hour time perspective. Ultrasound irradiation improved the epoxidation rate by facilitating the formation of a fine emulsion, that presumably enhanced the interfacial mass transfer. This led to an increase in the reaction rate of the perhydrolysis step where peroleic acid is formed from oleic acid and hydrogen peroxide. A top conversion value was reached after three hours of reaction with 90% amplitude of the ultrasound horn, and NMR analysis confirmed that there were no double bonds left after four hours of reaction. Furthermore, the concentration of epoxy groups was decreasing after four hours, and an accumulation of ring-opening products, predominantly consisting of esters, can be observed at longer reaction times. Hence, the reaction in the presence of ultrasound should be ended after four to five hours of reaction time to obtain the highest values of the desired product.

A temperature range of 30-60 ˚C was screened without larger differences in the reaction rate or conversion. Nevertheless, the solidification of epoxide led to operational issues in lower temperatures of 30 ˚C and 45 ˚C. Consequently, the temperatures 50 ˚C and 60 ˚C were used to keep the organic phase workable. Stirring rates of 500, 750 and 1000 rpm were compared, with analogous results in reaction rate and conversion.

The catalyst reusability is a main issue for the economic viability of using Novozym® 435 as a catalyst for the epoxidation of unsaturated fatty acids. A series of three successive experiments of reusing catalyst was performed in both silent and ultrasound modes. The results were promising, showing low signs of deactivation in both modes. However, the SEM images revealed that the catalyst morphology had been substantially impacted by the acoustic cavitation caused by ultrasound irradiation. It cannot either be disregarded that the catalyst reusability experiments were only partly conducted with reused catalyst, thus, the good results are potentially influenced by the fresh catalyst added to each reusability experiment. It would be desirable to study the reusability using only reused catalyst in order to obtain completely reliable results.

Four different reaction mechanisms for mathematical modelling were proposed, all of them reaching a good enough fit to describe the experimental data. However, the mechanisms including the perhydrolysis step gave the best representation of data. Also considering the already existing theory for lipase catalyzed chemo-enzymatic epoxidation, the perhydrolysis step is needed for the epoxidation reaction between oleic and peroleic acid. Nevertheless, the models without the perhydrolysis step showed also good fit and low parameter standard errors due to the simplicity of the models.

In conclusion, the chemo-enzymatic approach to epoxidation of unsaturated fatty acids assisted by ultrasound irradiation showed promising results. However, previous studies have indicated that a rapid addition of hydrogen peroxide can cause catalyst deactivation, therefore, a semibatch process where hydrogen peroxide is added during a longer time-period could be studied in the future. Experiments where a simple alkene, such as octane, dodecane or an ester of oleic acid without a carboxylic group, is exposed by hydrogen peroxide could give further answers whether a direct epoxidation of double bonds is possible to obtain without the perhydrolysis step. Additionally, analysis on the existence of peroleic acid during a typical chemo-enzymatic epoxidation experiment would presumably determine whether the reaction mechanism goes through the percarboxylic acid route or not.

Svensk sammanfattning – Swedish summary

Lipaskatalyserad kemisk-enzymatisk epoxidering av fettsyror med hjälp av ultraljud som en processintensifieringsmetod

Klimatförändringen har fört med sig nya utmaningar i att övergå från traditionella fossilt baserade naturresurser till förnybara resurser. Epoxidering av omättade, växtbaserade fettsyror är en metod som kan föra oss vidare mot en hållbar process inom kemikalietillverkning. Dessa epoxiderade oljor kan användas i produktionen av kemikalier som bland annat smörjmedel, mjukgörare i polymera produkter samt biobaserad och icke-isocyanatbaserad polyuretan. Omättade växtbaserade fettsyror härstammar vanligtvis från olika förnybara resurser som sojabönan, palm, raps, solrosfrön, linfrön och bomullsfrön. I Nordeuropa är tallolja, vilket är en biprodukt från sulfatprocessen i skogsindustrin, en stor hållbar råvara för vidareförädling till viktiga intermediära molekyler inom produktionen av förnybara kemikalier.

Detta arbete fokuserar på kemisk-enzymatisk epoxidering av oljesyra som en modellmolekyl, katalyserat av immobiliserat lipas. I motsats till den traditionella Prileschajews epoxideringsreaktionen av dubbelbindningar behövs ingen tillsatt karboxylsyra för att möjliggöra processen. Endast fettsyra, en oxidant som till exempel väteperoxid samt immobiliserat lipas behövs för att producera epoxiderade oljor enligt denna enzymatiska metod. Processförloppet sker i två steg: perhydrolys av fettsyrans karboxylgrupp till perfettsyra med hjälp av immobiliserat lipas, efterföljt av kemisk epoxidering av fettsyrans dubbelbindning med perfettsyran som nukleofil. Detta sker i ett trefassystem där perhydrolysen sker i vattenfasen och själva epoxideringsreaktionen mellan fettsyra och perfettsyra sker i den organiska fasen. Den intermediära massöverföringen mellan faserna möjliggörs genom att en gynnsam reaktionsomgivning bestående av en emulsion skapas.

Reaktionen intensifieras med hjälp av ultraljud vilket har en höjande effekt på reaktionshastigheten. Det intensifierande fenomenet grundar sig på akustisk kavitation, vilket innebär att små gasbubblor först skapas av ultraljud som växer större i systemet genom kompression och expansion. Detta leder slutligen till en snabb kollaps av bubblorna varefter lokala punkter med höga tryck och temperaturer skapas.

Fenomenet gör att massöverföringen mellan reaktionsfaserna intensifieras då en mer stabil emulsion skapas jämfört med en emulsion som skapas produceras enbart med omrörning i reaktorn.

En isotermisk satsreaktor med en roterande katalysatorbädd SpinChem® RBR samt ultraljudsanläggning insatt i reaktorn användes i samtliga experiment. Oljesyra och väteperoxid användes som reaktanter, och immobiliserat lipas (Novozym® 435) användes som katalysator. Reaktionskinetiken analyserades med titrimetriska metoder där icke-reagerade kvarstående fettsyra som reaktant (jodtalet, eng. Iodine value, enligt Hanus metod), koncentrationen epoxiderad fettsyra som produkt (oxiransyretalet, eng. Oxirane oxygen value, enligt Jays metod) samt koncentrationen väteperoxid (enligt Greenspan och MacKellars metod) analyserades under hela reaktionsförloppet i varje experiment. En ytterligare analys av den kemiska sammansättningen gjordes med kärnmagnetisk resonansspektroskopi (eng. Nuclear Magnetic Resonance spectroscopy, NMR) och katalysatorytans morfologi studerades med svepelektronmikroskopi (eng. Scanning Electron Microscopy, SEM).

Användningen av olika koncentrationsförhållanden väteperoxid och fettsyra studerades i kinetiska experiment utan ultraljud. I dessa experiment visade koncentrationsförhållandet mellan oljesyra och väteperoxid på 1:2 vara det mest effektiva med toppvärden i utbyte efter fyra timmars reaktion då både reaktionshastigheten och utbytet utvärderades.

Ultraljudets inverkan på reaktionens omsättning och produktselektivitet studerades genom att använda olika amplituder på 30 %, 60 % och 90 % med en frekvens på 20 kHz. Dessa experiment påvisade att den akustiska kavitationen orsakat av ultraljud har en klar positiv påverkan på reaktionshastigheten. Experimentet utfört med 90 % amplitud nådde sin topp i utbyte efter tre timmars reaktionstid. Dock kunde det inte observeras en märkbar skillnad i slutligt utbyte mellan epoxideringsreaktionen som utfördes i tysta förhållanden och de experiment som utfördes i närvaro av ultraljud.

Reaktionstemperaturens betydelse i ultraljudsförhållanden studerades. Tidigare studier har indikerat att katalysatorns stabilitet kan påverkas av temperaturer som överstiger 50 ºC samt av höga omrörningshastigheter. Temperaturens skadliga påverkan på enzymstabiliteten kunde inte påvisas i högre grad av de experiment som utfördes i detta arbete då experimentet i 60 ºC nådde de bästa resultaten i

reaktionshastighet och utbyte. Låga temperaturer på 45 ºC och 30 ºC ledde till att produkten övergick i fast fas före reaktionsförloppets planerade slut. Därmed kan det konstateras att lägre temperaturer kan orsaka begränsningar i massöverföringen mellan vattenfasen och organiska fasen i reaktionssystemet.

Tidigare studier har påvisat att höga omrörningshastigheter även kan påverka lipasens stabilitet, vilket kan leda till lägre reaktionshastigheter och utbyten. Med härledning till detta studerades olika hastigheter på 500 rpm, 750 rpm och 1000 rpm, varav 750 rpm visade sig vara den mest effektiva. Dock kunde det konstateras att en hög omrörningshastighet inte påverkar stabiliteten. Detta kan hypotetiskt vara på grund av användandet av SpinChem® RBR vars filter omkring omrörarbladen kan anses ge ett skydd för katalysatorns struktur.

Återanvändningen av katalysatorn är en väsentlig fråga för de ekonomiska aspekterna i att använda Novozym® 435 som immobiserad katalysator för epoxidering av omättade fettsyror. Detta studerades genom tre efterföljande experiment med återanvänd katalysator i både tysta förhållanden och ultraljudsförhållanden. Dessa experiment gav goda resultat med endast en liten minskning i reaktionshastigheten. SEM bilder av katalysatorn i experimenten som studerade återanvändbarheten av katalysatorn i ultraljudsförhållanden visade att katalysatorns yta förstördes av den akustiska kavitationen. Detta påverkade trots allt inte katalysatorns kemiska aktivitet.

Den kemiska sammansättningen av produkterna som erhölls i tysta förhållanden, ultraljudsförhållanden och från katalysatorns återanvändningsexperiment efter fyra och åtta timmars reaktionstid analyserades med ^{1}H-NMR. Resultaten visade att det inte finns resterande omättad fettsyra kvar i ett enda analyserat prov efter åtta timmars reaktionstid, vilket tyder på att ett fullständigt produktutbyte hade uppnåtts. Dock kunde ringöppningsbiprodukter hittas, bestående främst av estrar och en mindre mängd dioler. Dessa hade förmodligen bildats genom att fettsyrans karboxylgrupp samt vatten hade agerat som nukleofiler i processen. Andelen biprodukter var ändå relativt liten, i experimentet utfört i tysta förhållanden var andelen störst av alla analyserade experiment med en mängd på ungefär 10 %.

Fyra olika matematiska modeller för reaktionskinetiken skapades samt estimering av kinetiska och termodynamiska parametrar utfördes för att anpassa beräknade data med experimentella data under tysta förhållanden. Statistiskt kunde endast smärre skillnader ses mellan de olika modellerna, men kännedomen om de möjliga reaktionsmekanismerna gjorde en mekanism som inkluderar perfettsyra till den mest sannolika modellen.

Kemisk-enzymatisk epoxidering av omättande fettsyror med hjälp av immobiliserat lipas som katalysator visade lovande resultat både i experiment med ultraljud och utan ultraljud. Användningen av ultraljud visade sig vara gynnsamt med tanke på reaktionssystemets effektivitet. Katalysatorn visade sig vara återanvändbar i både tysta och ultraljudsförhållanden. I framtiden kunde det vara intressant att forska hur användandet av en halvkontinuerlig reaktor med en långsammare tillsättning av väteperoxid påverkar lipasens aktivitet och därmed även reaktionshastigheten och produktselektiviteten. Ett experiment där en enkel alken utan en karboxylsyragrupp såsom okten, dodeken eller oljesyrans ester skulle utsättas av väteperoxid med målet att epoxidera dubbelbindningen kunde ge svar huruvida epoxideringen kan ske genom en reaktionsmekanism som inte kräver persyra. Dessutom kunde existensen av peroljesyra i den kemisk-enzymatiska epoxideringsmekanismen bevisas genom titrimetisk analys under experimentets gång.

References

[1] T. M. Panchal, A. Patel, D. D. Chauhan, M. Thomas, and J. V. Patel, "A methodological review on bio-lubricants from vegetable oil based resources," *Renew. Sustain. Energy Rev.*, vol. 70, pp. 65–70, Apr. 2017, doi: 10.1016/j.rser.2016.11.105.

[2] L. H. Gan, K. S. Ooi, S. H. Goh, L. M. Gan, and Y. C. Leong, "Epoxidized esters of palm olein as plasticizers for poly(vinyl chloride)," *Eur. Polym. J.*, vol. 31, no. 8, pp. 719–724, Aug. 1995, doi: 10.1016/0014-3057(95)00031-3.

[3] A. Abolins, R. Pomilovskis, E. Vanags, I. Mierina, S. Michalowski, A. Fridrihsone, and M. Kirpluks, "Impact of Different Epoxidation Approaches of Tall Oil Fatty Acids on Rigid Polyurethane Foam Thermal Insulation," *Materials*, vol. 14, no. 4, p. 894, Feb. 2021, doi: 10.3390/ma14040894.

[4] W. Y. Pérez-Sena, X. Cai, N. Kebir, L. Vernières-Hassimi, C. Serra, T. Salmi, and S. Leveneur, "Aminolysis of cyclic-carbonate vegetable oils as a non-isocyanate route for the synthesis of polyurethane: A kinetic and thermal study," *Chem. Eng. J.*, vol. 346, pp. 271–280, Aug. 2018, doi: 10.1016/j.cej.2018.04.028.

[5] BCC research LLC, "Oleochemical Fatty Acids: Global Markets to 2023," CHM062E, Jan. 2019. Accessed: Feb. 25, 2021. [Online]. Available: https://academic.bccresearch.com/market-research/chemicals/oleochemical-fatty-acids-global-markets.html.

[6] S. M. Danov, O. A. Kazantsev, A. L. Esipovich, A. S. Belousov, A. E. Rogozhin, and E. A. Kanakov, "Recent advances in the field of selective epoxidation of vegetable oils and their derivatives: a review and perspective," *Catal. Sci. Technol.*, vol. 7, no. 17, pp. 3659–3675, 2017, doi: 10.1039/C7CY00988G.

[7] V. Aryan and A. Kraft, "The crude tall oil value chain: Global availability and the influence of regional energy policies," *J. Clean. Prod.*, vol. 280, p. 124616, Jan. 2021, doi: 10.1016/j.jclepro.2020.124616.

[8] A. F. Aguilera, J. Rahkila, J. Hemming, M. Nurmi, G. Torres, T. Razat, P. Tolvanen, K. Eränen, S. Leveneur, and T. Salmi, "Epoxidation of Tall Oil Catalyzed by an Ion Exchange Resin under Conventional Heating and Microwave Irradiation," *Ind. Eng. Chem. Res.*, vol. 59, no. 22, pp. 10397–10406, Jun. 2020, doi: 10.1021/acs.iecr.0c01288.

[9] M. Kirpluks, E. Vanags, A. Abolins, A. Fridrihsone, and U. Cabulis, "Chemo-enzymatic oxidation of tall oil fatty acids as a precursor for further polyol production," *J. Clean. Prod.*, vol. 215, pp. 390–398, Apr. 2019, doi: 10.1016/j.jclepro.2018.12.323.

[10] C. Orellana-Coca, S. Camocho, D. Adlercreutz, B. Mattiasson, and R. Hatti-Kaul, "Chemo-enzymatic epoxidation of linoleic acid: Parameters influencing the reaction," *Eur. J. Lipid Sci. Technol.*, vol. 107, no. 12, pp. 864–870, Dec. 2005, doi: 10.1002/ejlt.200500253.

[11] T. Vlcek and Z. S. Petrovic, "Optimization of the Chemoenzymatic Epoxidation of Soybean Oil," *J. Am. Oil Chem. Soc.*, vol. 83, pp. 247–252, Mar. 2006.

[12] M. S. Bhalerao, V. M. Kulkarni, and A. V. Patwardhan, "Ultrasound-assisted chemoenzymatic epoxidation of soybean oil by using lipase as biocatalyst," *Ultrason. - Sonochemistry*, vol. 40, pp. 912–920, Jan. 2017, doi: 10.1016/j.ultsonch.2017.08.042.

[13] X. Zhang, J. Burchell, and N. S. Mosier, "Enzymatic Epoxidation of High Oleic Soybean Oil," *ACS Sustain. Chem. Eng.*, vol. 6, no. 7, pp. 8578–8583, Jul. 2018, doi: 10.1021/acssuschemeng.8b00884.

[14] R. de C. S. Schneider, L. R. S. Lara, T. B. Bitencourt, M. da G. Nascimento, and M. R. dos S. Nunes, "Chemo-enzymatic epoxidation of sunflower oil methyl esters," *J. Braz. Chem. Soc.*, vol. 20, no. 8, pp. 1473–1477, 2009, doi: 10.1590/S0103-50532009000800013.

[15] I. Hilker, D. Bothe, J. Prüss, and H.-J. Warnecke, "Chemo-enzymatic epoxidation of unsaturated plant oils," *Chem. Eng. Sci.*, vol. 56, no. 2, pp. 427–432, Jan. 2001, doi: 10.1016/S0009-2509(00)00245-1.

[16] S. Warwel and M. Rüsch gen. Klaas, "Chemo-enzymatic epoxidation of unsaturated carboxylic acids," *J. Mol. Catal. B Enzym.*, vol. 1, no. 1, pp. 29–35, Dec. 1995, doi: 10.1016/1381-1177(95)00004-6.

[17] N. Prileschajew, "Oxydation ungesättiger Verbindungen mittels organischer Superoxyde," *Berichte Dtsch. Chem. Ges.*, vol. 42, no. 4, pp. 4811–4815, Dec. 1909, doi: 10.1002/cber.190904204100.

[18] S. Leveneur, A. Ledoux, L. Estel, B. Taouk, and T. Salmi, "Epoxidation of vegetable oils under microwave irradiation," *Chem. Eng. Res. Des.*, vol. 92, no. 8, pp. 1495–1502, Aug. 2014, doi: 10.1016/j.cherd.2014.04.010.

[19] A. F. Aguilera, P. Tolvanen, K. Eränen, S. Leveneur, and T. Salmi, "Epoxidation of oleic acid under conventional heating and microwave radiation," *Chem. Eng. Process.*, vol. 102, pp. 70-87, 2016, doi:10.1016/j.cep.2016.01.011

[20] S. Dinda, A. V. Patwardhan, V. V. Goud, and N. C. Pradhan, "Epoxidation of cottonseed oil by aqueous hydrogen peroxide catalysed by liquid inorganic acids," *Bioresour. Technol.*, vol. 99, no. 9, pp. 3737–3744, Jun. 2008, doi: 10.1016/j.biortech.2007.07.015.

[21] A. F. Aguilera, P. Tolvanen, A. Oger, K. Eränen, S. Leveneur, J. P. Mikkola, and T. Salmi, "Screening of ion exchange resin catalysts for epoxidation of oleic acid under the influence of conventional and microwave heating," *J Chem Technol Biotechnol*, vol. 94, pp. 3020-3031 , Jul. 2019, doi: 10.1002/jctb.6112.

[22] A. F. Aguilera, P. Tolvanen, S. Heredia, M. G. Muñoz, T. Samson, A. Oger, A. Verove, K. Eränen, S. Leveneur, J. P. Mikkola, and T. Salmi, "Epoxidation of Fatty Acids and Vegetable Oils Assisted by Microwaves Catalyzed by a Cation Exchange Resin," *Ind. Eng. Chem. Res.*, vol. 57, no. 11, pp. 3876–3886, Mar. 2018, doi: 10.1021/acs.iecr.7b05293.

[23] X. Cai, J. L. Zheng, A. F. Aguilera, L. Vernièrez-Hassimi, P. Tolvanen, T. Salmi, S. Leveneur, "Influence of ring-opening reactions on the kinetics of cottonseed oil epoxidation," *Int. J. Chem. Kinet.*, vol. 50, no. 10, pp. 726–741, Oct. 2018, doi: 10.1002/kin.21208.

[24] F. Björkling, S. E. Godtfredsen, O. Kirk, "Lipase-mediated formation of peroxycarboxylic acids used in catalytic epoxidation of alkenes," *J. Chem. Soc. Chem. Commun.*, vol. 19, pp. 1301-1303, 1990, doi: 10.1039/C39900001301.

[25] M. Rüsch gen. Klaas and S. Warwel, "Complete and partial epoxidation of plant oils by lipase-catalyzed perhydrolysis," *Ind. Crops Prod.*, vol. 9, no. 2, pp. 125–132, Jan. 1999, doi: 10.1016/S0926-6690(98)00023-5.

[26] G. D. Yadav and K. Manjula Devi, "A kinetic model for the enzyme-catalyzed self-epoxidation of oleic acid," *J. Am. Oil Chem. Soc.*, vol. 78, no. 4, pp. 347–351, Apr. 2001, doi: 10.1007/s11746-001-0267-2.

[27] U. Törnvall, C. Orellana-Coca, R. Hatti-Kaul, and D. Adlercreutz, "Stability of immobilized Candida antarctica lipase B during chemo-enzymatic epoxidation of fatty acids," *Enzyme Microb. Technol.*, vol. 40, no. 3, pp. 447–451, Feb. 2007, doi: 10.1016/j.enzmictec.2006.07.019.

[28] P. Anastas and N. Eghbali, "Green Chemistry: Principles and Practice," *Chem Soc Rev*, vol. 39, no. 1, pp. 301–312, 2010, doi: 10.1039/B918763B.

[29] C. Orellana-Coca, U. Törnvall, D. Adlercreutz, B. Mattiasson, and R. Hatti-Kaul, "Chemo-enzymatic epoxidation of oleic acid and methyl oleate in solvent-free medium," *Biocatal. Biotransformation*, vol. 23, no. 6, pp. 431–437, Jan. 2005, doi: 10.1080/10242420500389488.

[30] C. Aouf, E. Durand, J. Lecomte, M. Figueroa-Espinoza, E. Dubreucq, H. Fulcrand, and P. Villeneuve, "The use of lipases as biocatalysts for the epoxidation of fatty acids and phenolic compounds," *Green Chem*, vol. 16, no. 4, pp. 1740–1754, 2014, doi: 10.1039/C3GC42143K.

[31] A. F. Aguilera, P. Tolvanen, V. S. Herrera, J.-N. Tourvielle, S. Leveneur, and T. Salmi, "Reaction intensification by microwave and ultrasound techniques in chemical multiphase systems," in *Process Synthesis and Process Intensification: Methodological Approaches*, Walter de Gruyter GmbH & Co KG, 2017, pp. 111–142.

[32] A. F. Aguilera, "Epoxidation of vegetable oils : process intensification for biomass conversion," Doctoral Thesis, Åbo Akademi University, Turku, Finland, 2020.

[33] H. Mallin, J. Muschiol, E. Byström, and U. T. Bornscheuer, "Efficient Biocatalysis with Immobilized Enzymes or Encapsulated Whole Cell Microorganism by Using the SpinChem Reactor System," *ChemCatChem*, vol. 5, no. 12, pp. 3529–3532, Dec. 2013, doi: 10.1002/cctc.201300599.

[34] S. Pithani, S. Karlsson, H. Emtenäs, and C. T. Öberg, "Using Spinchem Rotating Bed Reactor Technology for Immobilized Enzymatic Reactions: A Case Study," *Org. Process Res. Dev.*, vol. 23, no. 9, pp. 1926–1931, Sep. 2019, doi: 10.1021/acs.oprd.9b00240.

[35] K. S. Suslick, "The Chemical Effects of Ultrasound," *Sci. Am.*, vol. 260, no. 2, pp. 80–86, Feb. 1989, doi: 10.1038/scientificamerican0289-80.

[36] P. R. Gogate, S. Mujumdar, and A. B. Pandit, "Large-scale sonochemical reactors for process intensification: design and experimental validation," *J. Chem. Technol. Biotechnol.*, vol. 78, no. 6, pp. 685–693, Jun. 2003, doi: 10.1002/jctb.697.

[37] I. Gonçalves, C. Silva, and A. Cavaco-Paulo, "Ultrasound enhanced laccase applications," *Green Chem.*, vol. 17, no. 3, pp. 1362–1374, 2015, doi: 10.1039/C4GC02221A.

[38] L. H. Thompson and L. K. Doraiswamy, "Sonochemistry: Science and Engineering," *Ind. Eng. Chem. Res.*, vol. 38, no. 4, pp. 1215–1249, Apr. 1999, doi: 10.1021/ie9804172.

[39] S. H. Lee, H. M. Nguyen, Y.-M. Koo, and S. H. Ha, "Ultrasound-enhanced lipase activity in the synthesis of sugar ester using ionic liquids," *Process Biochem.*, p. 4, 2008.

[40] L. A. Lerin, R. A. Loss, D. Remonatto, M. C. Zenevicz, M. Balen, V. O. Netto, J. L. Ninow, C. M. Trentin, and J. V. de Oliveira, "A review on lipase-catalyzed reactions in ultrasound-assisted systems," *Bioprocess Biosyst. Eng.*, vol. 37, no. 12, pp. 2381–2394, Dec. 2014, doi: 10.1007/s00449-014-1222-5.

[41] F. P. Greenspan and D. G. MacKellar, "Analysis of Aliphatic Per Acids," *Anal. Chem.*, vol. 20, no. 11, pp. 1061–1063, 1948.

[42] C. Paquot, "Determination of the Iodine Value (I.V.)," in *Standard Methods for the Analysis of Oils, Fats and Derivatives*, Elsevier, 1979, pp. 66–70.

[43] R. R. Jay, "Direct Titration of Epoxy Compounds and Aziridines.," *Anal. Chem.*, vol. 36, no. 3, pp. 667–668, 1964, doi: 10.1021/ac60209a037.

[44] W. Y. Pérez-Sena, T. Salmi, L. Estel, and S. Leveneur, "Thermal risk assessment for the epoxidation of linseed oil by classical Prisleschajew epoxidation and by direct epoxidation by H2O2 on alumina," *J. Therm. Anal. Calorim.*, vol. 140, no. 2, pp. 673–684, Apr. 2020, doi: 10.1007/s10973-019-08894-2.

[45] D. Marquardt, "An Algorithm for Least-Squares Estimation of Nonlinear Parameters," *J. Soc. Ind. Appl. Math.*, vol. 11, no. 2, pp. 431–441, 1963, doi: 10.1137/0111030.

[46] J. Vojtesek, "Numerical Solution of Ordinary Differential Equations Using Mathematical Software," in *Modern Trends and Techniques in Computer Science. Advances in Intelligent Systems and Computing*, Springer, Cham, May. 2014, pp. 213–226, doi: 10.1007/978-3-319-06740-7_19.

[47] J. R. Dormand and P. J. Prince, "A family of embedded Runge-Kutta formulae," *J. Comput. Appl. Math.*, vol. 6, no. 1, pp. 19–26, Mar. 1980, doi: 10.1016/0771-050X(80)90013-3.

[48] A. F. Aguilera, P. Tolvanen, K. Eränen, J. Wärnå, S. Leveneur, T. Marchant, and T. Salmi, “Kinetic modelling of Prileschajew epoxidation of oleic acid under conventional heating and microwave irradiation,” *Chem. Eng. Sci.*, vol. 199, pp. 426-438, May. 2019, doi: 10.1016/j.ces.2019.01.035.

Appendices

Appendix I

Figure Appendix I 1 - Analysis equipment for iodine value titrations with sodium thiosulphate

Figure Appendix I 2 - Analysis equipment for oxirane number titrations with perchloric acid

Figure Appendix I 3 - Analysis equipment for hydrogen peroxide titrations with ammonium cerium sulfate

Figure Appendix I 4 - Image of the isothermal batch reactor system with the ultrasound probe in use

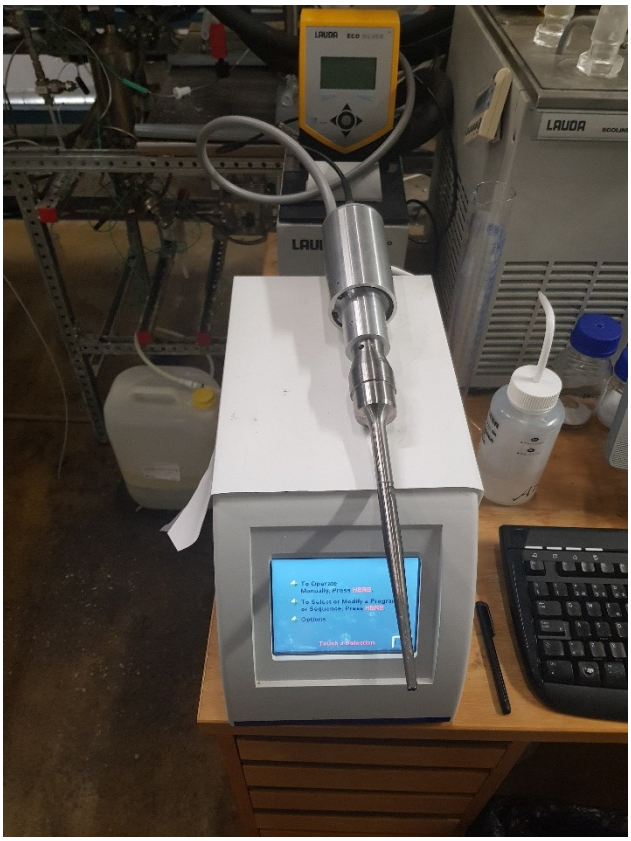

Figure Appendix I 4 – Image of the ultrasound horn equipment

Appendix II

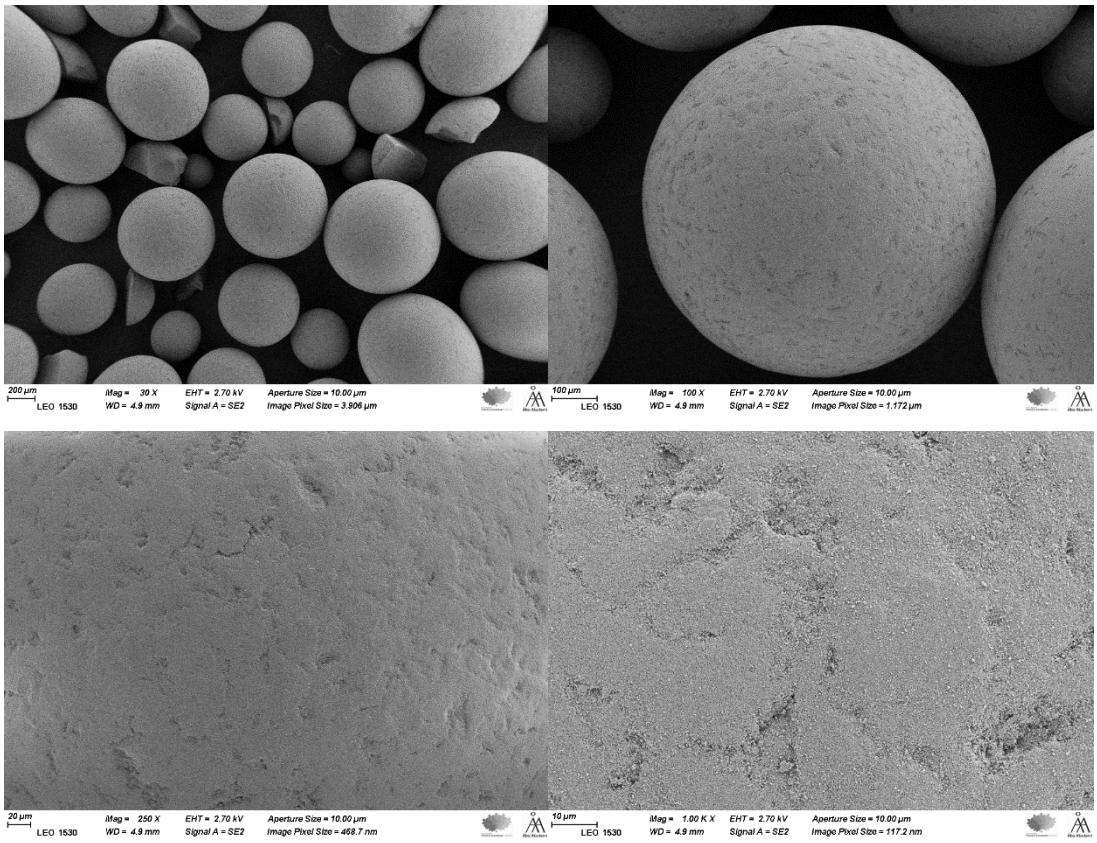

Figure Appendix II 1 - SEM images (30x, 100x, 250x, and 1000x size from left to right, accordingly) from unused immobilized lipase Novozym 435

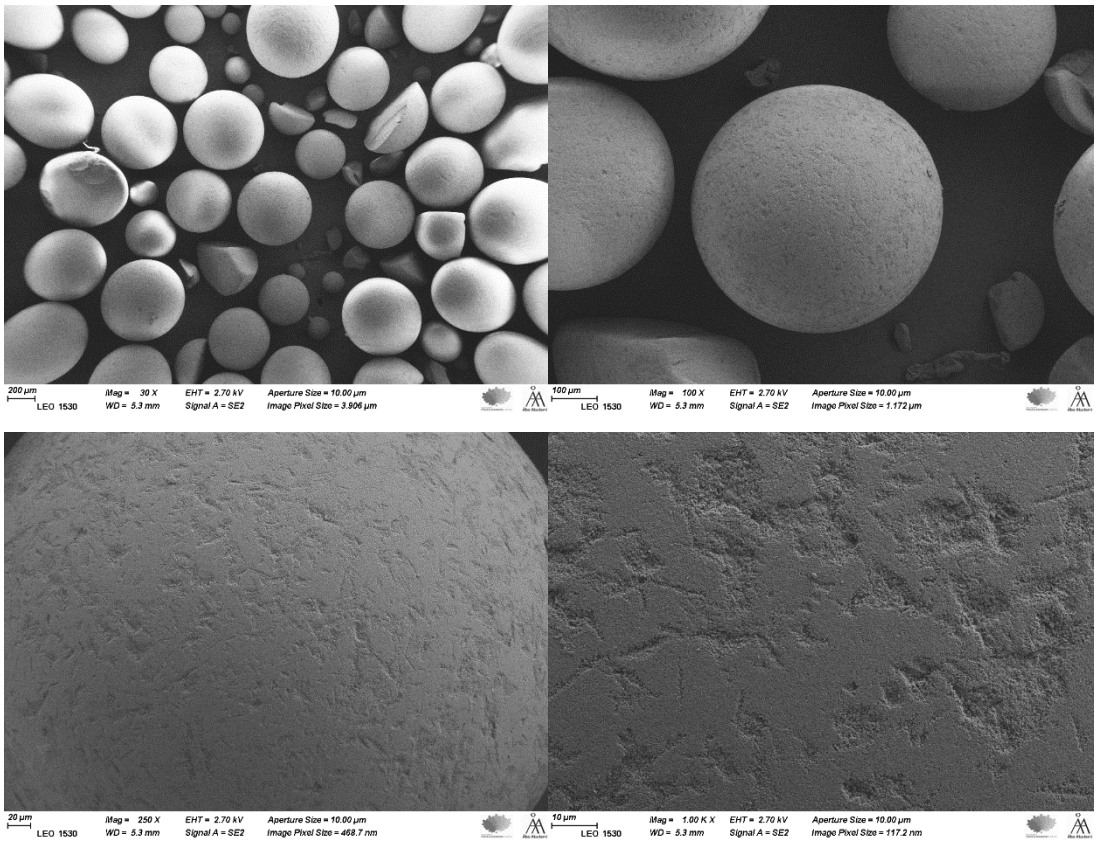

Figure Appendix II 2 - SEM images (30x, 100x, 250x, and 1000x size from left to right, accordingly) from immobilized lipase Novozym 435 used once in silent mode[i]

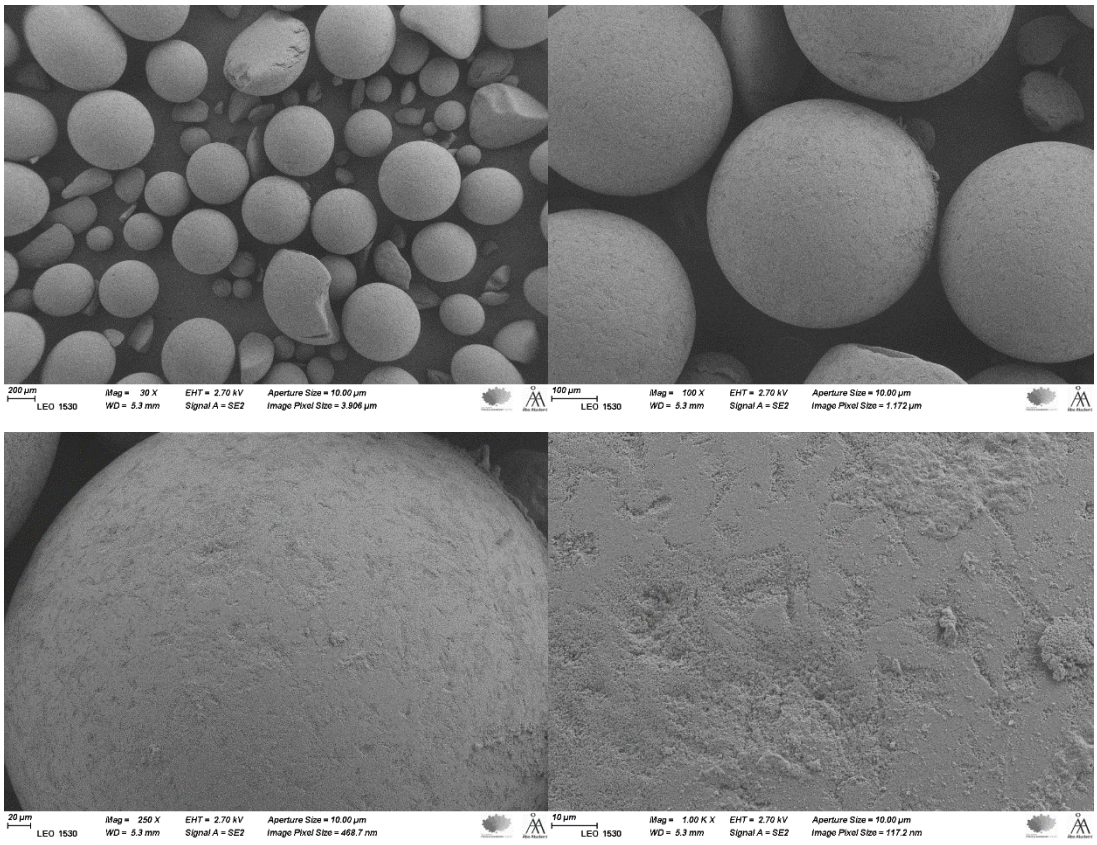

Figure Appendix II 3 - SEM images (30x, 100x, 250x, and 1000x size from left to right, accordingly) from immobilized lipase Novozym 435 used twice in silent mode

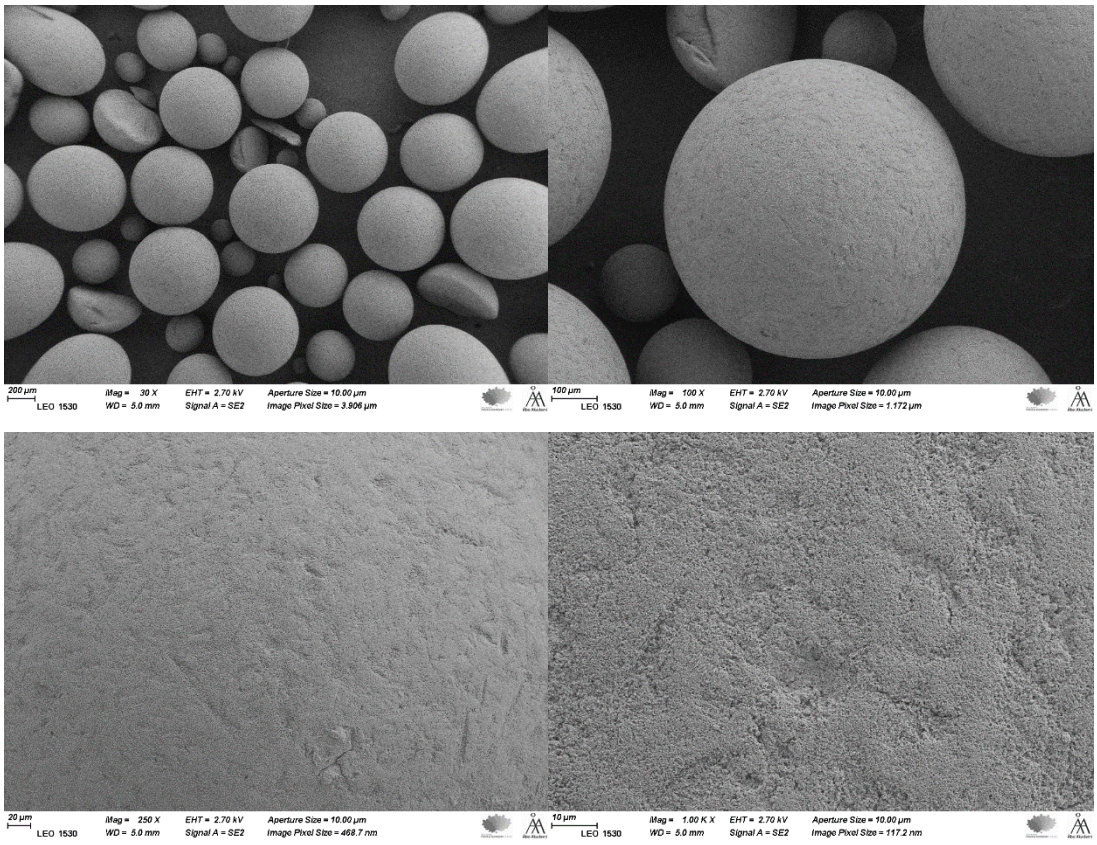

Figure Appendix II 4 - SEM images (30x, 100x, 250x, and 1000x size from left to right, accordingly) from immobilized lipase Novozym 435 after three consecutive uses in silent mode

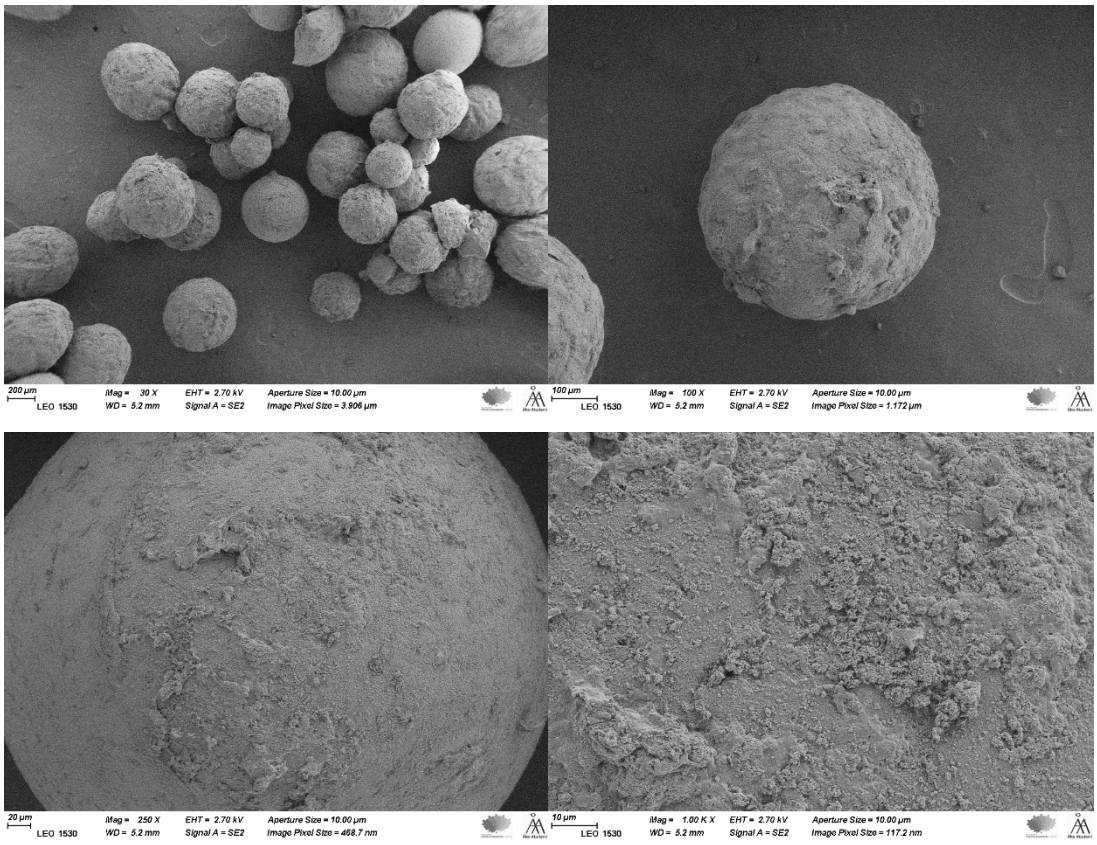

Figure Appendix II 5 - SEM images (30x, 100x, 250x, and 1000x size from left to right, accordingly) from immobilized lipase Novozym 435 after one use with ultrasound irradiation

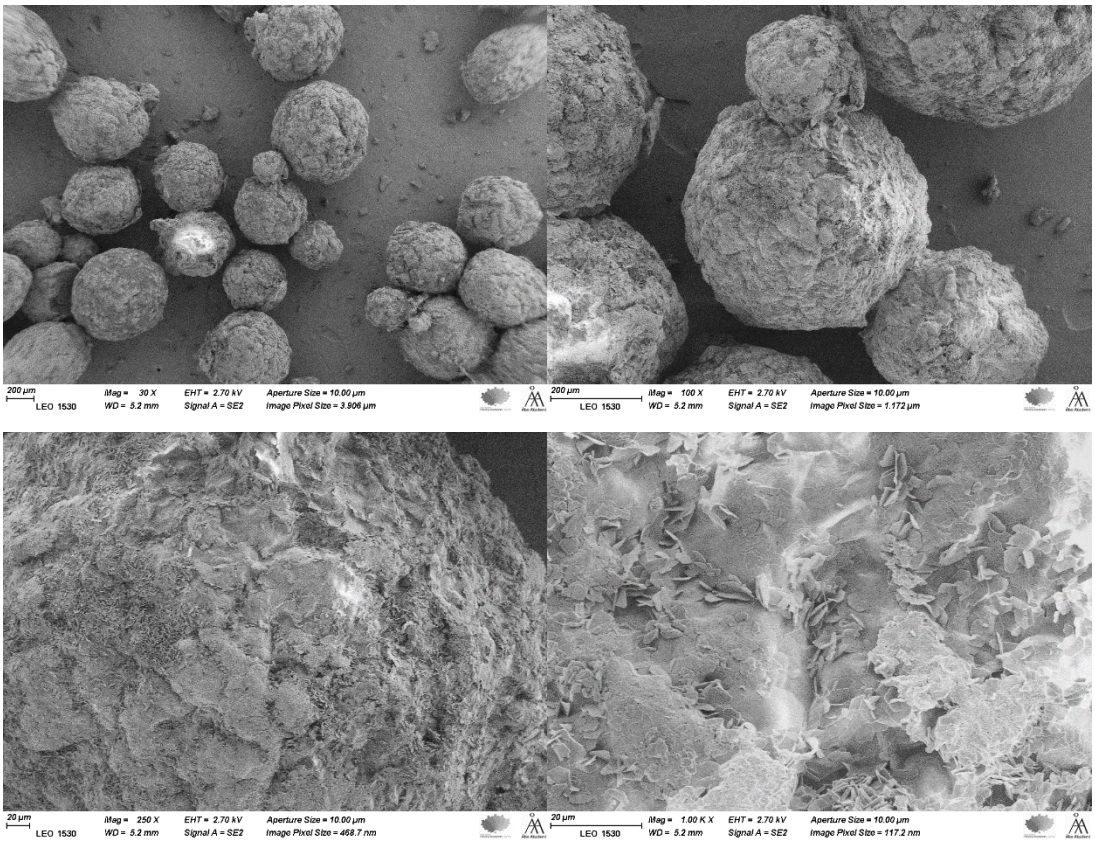

Figure Appendix II 6 - SEM images (30x, 100x, 250x, and 1000x size from left to right, accordingly) from immobilized lipase Novozym 435 after two consecutive uses with ultrasound irradiation

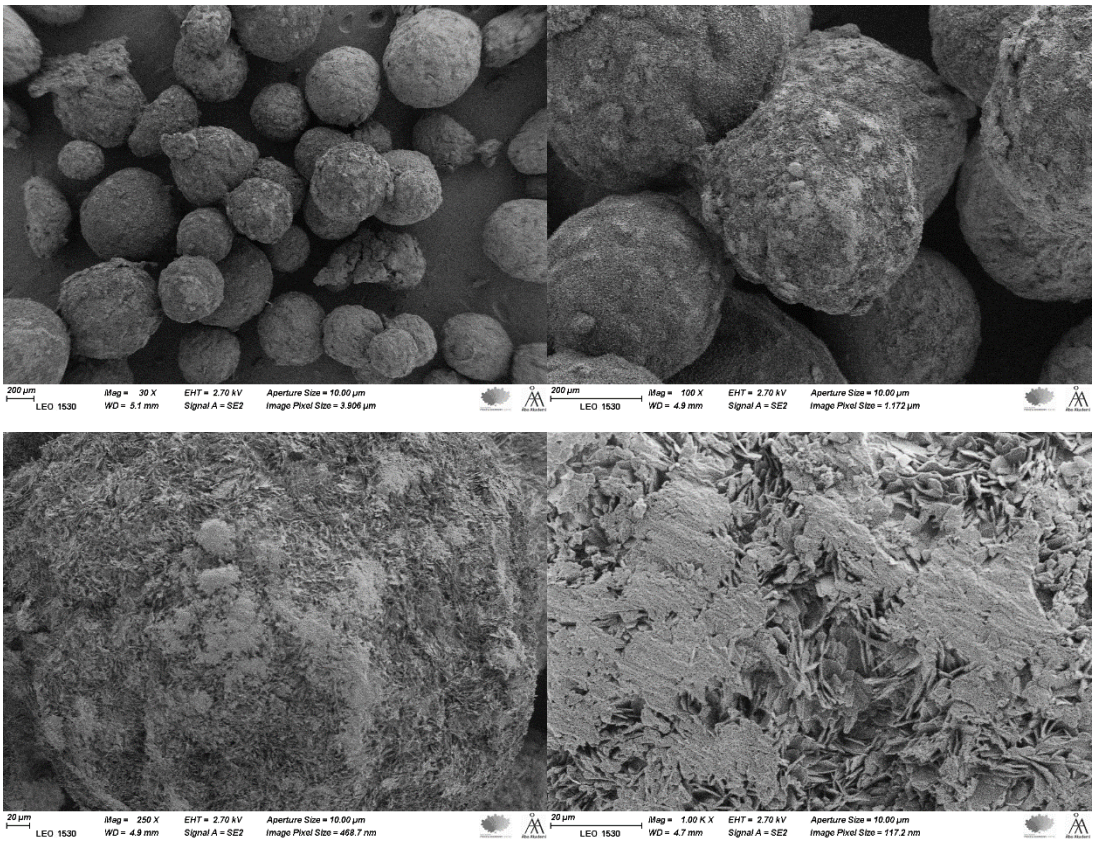

Figure Appendix II 7 - SEM images (30x, 100x, 250x, and 1000x size from left to right, accordingly) from immobilized lipase Novozym 435 after three consecutive uses with ultrasound irradiation